University of Alberta

Monitoring of Celullar and Subcellular Properties on a Microchip

by

Jelena Dragoljic

A thesis submitted to the Faculty of Graduate Studies and Research in partial fulfillment of the requirements for the degree of Master of Science.

Department of Chemistry
Edmonton, Alberta
Spring 2004

Library and Archives Canada

Published Heritage Branch

395 Wellington Street
Ottawa ON K1A 0N4
Canada

Bibliothèque et Archives Canada

Direction du Patrimoine de l'édition

395, rue Wellington
Ottawa ON K1A 0N4
Canada

Your file Votre référence
ISBN: 0-612-96469-8
Our file Notre référence
ISBN: 0-612-96469-8

The author has granted a non-exclusive license allowing the Library and Archives Canada to reproduce, loan, distribute or sell copies of this thesis in microform, paper or electronic formats.

The author retains ownership of the copyright in this thesis. Neither the thesis nor substantial extracts from it may be printed or otherwise reproduced without the author's permission.

L'auteur a accordé une licence non exclusive permettant à la Bibliothèque et Archives Canada de reproduire, prêter, distribuer ou vendre des copies de cette thèse sous la forme de microfiche/film, de reproduction sur papier ou sur format électronique.

L'auteur conserve la propriété du droit d'auteur qui protège cette thèse. Ni la thèse ni des extraits substantiels de celle-ci ne doivent être imprimés ou aturement reproduits sans son autorisation.

In compliance with the Canadian Privacy Act some supporting forms may have been removed from this thesis.

While these forms may be included in the document page count, their removal does not represent any loss of content from the thesis.

Conformément à la loi canadienne sur la protection de la vie privée, quelques formulaires secondaires ont été enlevés de cette thèse.

Bien que ces formulaires aient inclus dans la pagination, il n'y aura aucun contenu manquant.

Canada

Abstract

This work focuses on the design and testing of a microchip that operates in a "flow cytometry-like" format. Microfluidic devices were used in combination with a fluorescence detection system. A multi-wavelength detection system was built and optimized conditions for data collection were obtained by adjusting LabView and Origin 7.0 software to suit the experimental conditions. We also developed an "in-house" procedure for isolation of mitochondria from Jurkat cells. Once the equipment was ready, we tested it by performing dose and time response studies, treating Jurkat cells and isolated mitochondria with valinomycin and oligomycin. Mitochondria membrane potential ($\Delta\Psi_M$) changes were monitored with JC-1 staining, which indicates changes in polarization of mitochondria membranes after drug treatment. The same type of studies was performed using the conventional technique, flow cytometry, and the results were compared with those obtained using the chip and multi-wavelength detection system. Our results demonstrate that microchip with a multi-wavelength detection system and flow cytometry gave similar results.

To My Dear Parents

Branislava and Stanimir

Acknowledgements

I would sincerely like to thank to my supervisor, Dr. Jed Harrison, who guided my research and offered his help whenever I needed it. It was a pleasure working in his lab and learning about microfludics, which I had not been familiar with before I joined his group. I especially appreciate that he provides funding for all his students to attend conferences, which are a great learning source.

Working on my project, I often needed the assistance of experts. I give special thanks to Dr. Sandra Marcus, who put a lot of work into helping me to isolate mitochondria. We spent many hours in the lab and it was always pleasant working with her. I also want to acknowledge to Randy Tsen, who wrote the software I used for data collection. Then, I thank to the technical support staff from the Nanofab, Machine Shop, Glass Shop and Electronic Shop (especially to Kim Nguy). Thanks to my defense examiners Dr. John-Bruce Green and Dr. Frank Nargang for useful discussions regarding my work.

Members of the Harrison group made my stay in the group enjoyable, and they were also very helpful whenever I was dealing with different problems related to my project. I particularly want to mention Justine for offering her help many times, Vasili for teaching me to culture cells, James Bao for working on my detection system, as well as Guifang, James Kariuki, Ehsan, Kowlasar and Dolores for the many useful discussions we had. I also give special thanks to Arlene Figley, who helped me organizing many different things.

Last, but not the least, I want to thank to my husband and my family for their moral support and care.

Table of Contents

Chapter 1 : Introduction 1
1.1 Introduction 1
1.2 Cells in Microfluidics (review) 2
1.2.1 Flow cytometry on chip 2
1.2.2 Monitoring of cells in steady state 4
1.2.3 Metabolic Monitoring 9
1.2.4 Cell Based Drug Screening and Tumor Pathology on Chip 14
1.3 Mitochondria and Apoptosis 17
1.3.1 Mitochondria 17
1.3.2 The Role of Mitochondria in Apoptosis 18
1.4 Overview of the Methods Used to Characterize Mitochondria Properties 19
1.5 Monitoring Mitochondria Membrane Potential as a Tool in Drug Trials 20
1.6 Scope of the Thesis 22
1.7 Bibliography 23
Chapter 2 : Preliminary Experimental 33
2.1 Introduction 33
2.2 Background Information on Reagents 34
2.2.1 Biological Samples 34
2.2.2 Sytox Green and JC-1 stain 41
2.2.3 Drugs Used for Treatment of Cells and Isolated Mitochondria 40
2.3 Experimental 42
2.3.1 Microfluidic device 42
2.3.2 Experimental Set Up 44
2.3.3 Reagents and Chemicals 48
2.3.4 Cell Culture 49
2.3.5 Mitochondria Isolation 49
2.3.6 Cell Viability 53
2.3.7 Test Experiments for monitoring $\Delta\psi_M$ 54
2.3.8 Data Capture and Analysis 55
2.4 Results and discussion 56
2.4.1 Mitochondria Isolation 56
2.4.2 Cell Viability 58
2.4.3 Test Experiments for Monitoring Mitochondria Membrane Potential 60
2.4.4 Data capture and Analysis 62
2.5 Conclusion 66
2.6 Bibliography 67
Chapter 3 : Monitoring of Mitochondria Membrane Potential 69
3.1 Introduction 69
3.1.1 The Goal of Our Experiments 69
3.2 Experimental 70
3.2.1 Sample Preparation 70
3.2.2 Experimental procedure 71
3.3 Results and Discussion 73

3.3.1 Chip Studies 73
3.3.2 Flow Cytometry Studies 82
3.3.3 Microchip/ Flow Cytometry Comparison 84
3.4 Conclusion 89
3.5 Bibliography 91
Chapter 4 : Summary 93
4.1 Summary 93
4.2 Bibliography 95
Appendix 96

List of Tables

Chapter 2

Page

Table 2-1. Emission wavelengths of three forms of CBB G-250.....50
Table 2-2. The temperature program for thermal bonding 57
Table 2-3 The results from the Bradford and succinate dehydrogenase assay for all the mitochondria samples we used in the experiments.....71
Table 2-4. PMT voltages and amplifier gains that are most appropriate for the experiments of $\Delta\psi_M$ monitoring in cells and isolated mitochondria.....79

Chapter 3

Table 3-1. Flow cytometer parameters 87
Table 3-2. Values from dose response studies shown in Figure3-4 95
Table 3-3. Time response study; flow cytometry experiment 97
Table 3-4. Time response study; microchip experiment 97

List of Figures

Chapter 1

Page

Figure 1-1. Hydrodynamic focusing effect of the micromachined flow cytometer.....11
Figure 1-2. Orientation angle for BAECs cultured in microchannels as a Function of microchannel width.....14
Figure 1-3. Normalized differences ΔZ, ΔR and ΔB, for each concentration of L, Innocua.....16

Chapter 2

Figure 2-1. Structural formula of CBB G-250.....45
Figure 2-2 Oxidation of succinate to fumarate.....46
Figure 2-3. Structural formula of INT molecule 47
Figure 24. Structural formula of JC-1 molecule.....48
Figure 2-5. Structure of Valinomycin molecule.....49
Figure 2-6. Structure of Oligomycin molecule.....50
Figure 2-7 Layout of the PCRD1 device.....51
Figure 2-8. Shematic layout of the part that connects PMTs with confocal microscope in multiwavelentgh detection system 55
Figure 2-9. Experimental set up.....56
Figure 2-10. Mitochondria Isolation on Percoll Gradient.....65
Figure 2-11. Trace of dead Jurkat cells stained with 1 μM Sytox Green.....68
Figure 2-12. Dead Jurkat cells flowing through the 70 μm deep microchannels..... 68
Figure 2-13. Green fluorescent signal from Jurkat cells treated with 70% ethanol and stained with JC-1..... 71
Figure 3-9. Comparative dose response study for microchip and flow cytometry.....96
Figure 2-14. Red fluorescent signal from Jurkat cells treated with 70% ethanol and stained with JC-1..... 71
Figure 2-15. The picture of stained healthy mitochondria within whole Jurkat cell.....71
Figure 2-16. Oscilloscope trace of green fluorescent signal from healthy Jurkat cells stained with JC-1.....73
Figure 2-17. Oscilloscope trace showing green fluorescent signal from healthy crude mitochondria stained with JC-1.....74

Chapter 3

Figure3-1. Traces of red and green fluorescence of crude mitochondria..... 84
Figure 3-2. Traces of red and green fluorescence for the control group and for drug treated mitochondria.....86
Figure 3-3. Comparison of data between intact cells and isolated mitochondria.....87
Figure 3-4. Comparative dose response studies for oligomycin and valinomycin (chip study).....90
Figure 3-5. Scattering plots of red vs. green fluorescence for isolated mitochondria treated with oligomycin 91
Figure 3-6. Comparative dose response for valinomycin and oligomycin (flow cytometry study)..... 92
Figure 3-7. Scatter plots of red vs. green fluorescence from comparative dose response study (flow cytometry).....93
Figure 3-8. Comparative time response study done with microchip and flow cytometer 94
Figure 3-10. Dose response study performed with isolated mitochondria and oligomycin (chip and flow cytometry comparison).....98
Figure 3-11. Dose response study with oligomycin 99

List of Abbreviations

AIF	Apoptosis Inducing Factor
ATP	Adenosine Triphosphate
ATTC	American Type Culture Collection
BAECs	Bovine Aortic Endothelial Cells
BSA	Bovine Serum Albumine
CBB	Coomasie Brilliant Blue
CE	Capillary Electrophoresis
DEP	Dielectrophoresis
$DiOC_6$	3, 3'- Dihexyloxacarbocyanine Iodide
EC	Endothelial Cell
EDTA	Ethylenedinitrilotetraacetic Acid
ER	Estrogen Receptor
FACS	Fluorescence Activated Cell Sorting
FAD	Flavine Adenine Dinucleoside
FAF-BSA	Fatty Acid Free Bovine Serum Albumin
FDG	Fluorescein - di - β - D - Galactopiranoside
f-MLP	Formyl - Met - Leu – Phe
GFP	Green Fluorescent Protein
HB	Homogenization Buffer
INT	Iodonitrotetrazolium Chloride
LIF	Laser Induced Fluorescence
MA	Mefenamic Acid
MACS	Magnetic Activated Cell Sorting
MIB	Mitochondria Buffer
MOPS	3-(N-Morpholino) Propanesulfonic Acid
PBS	Phosphate Buffered Saline
PCR	Polymerase Chain Reaction

PDMS	Polydimethylsiloxane
PMT	Photomultipler Tube
rpm	Revolutions Per Minute
RPMI	Roswell Park Memorial Institute
SDS	Sodium Dodecyl Sulphate
TMR	Tetramethylrhodamine
TNF	Tumor Necrosis Factor
TPP^+	Tetraphenyl Phosphonium Ion
TRβ	Thyroid Hormone Receptor β
TRAIL	Tumor Necrosis Factor - Related Apoptosis Inducing Ligand

Chapter 1: Introduction

1.1 Introduction

This thesis presents work on monitoring cellular and subcellular components on microfluidic devices that operate in a "flow-cytometry-like" format. In order to test our device, we have chosen to analyze one of the key apoptosis indicators: mitochondrial membrane potential ($\Delta\psi_M$). The introductory chapter provides a review of previous research on the use of microfluidics for the analysis of different cell properties. It summarizes up-to-date studies about flow cytometry on chip, analysis of cellular physical properties and metabolic monitoring, cell-based drug screening and tumor pathology. There is also a brief overview of mitochondrial properties, their role in apoptosis, and the helpfulness of monitoring $\Delta\psi_M$ in drug trials; including the techniques that are used to do so. The remaining chapters describe the design and development of a microfluidic system for flow cytometry, and its application to the analysis of mitochondria membrane potential as a result of exposure to different drugs. The microchip approach is then compared to a flow cytometer by evaluating studies with both systems.

1.2 Cells in Microfluidics (review)

Over the past decade, microchip-based systems have been developed very intensively. There are a large number of reviews that summarize the latest achievements in microfluidics. They focus on different aspects, such as reactions and separations [1], cell studies [2, 3], high-throughput screening [3-5], miniaturized capillary electrophoresis (CE) systems [6-8] and cytometry [9, 10]. We focus our discussion on cell studies in microfluidics, examining a few aspects relevant to this thesis: flow cytometry on chip, analysis of a cell's physical properties in steady state, metabolic monitoring of a cell, cell -based drug screening and tumor pathology on chip. Most of these sections present the achievements in chronological order, giving a sense of the research dynamics for a specific area.

1.2.1 Flow Cytometry On Chip

Conventional flow cytometers are widely used for cell studies. Cell sorting can use fluorescence activated cell sorting (FACS) or magnetic activated cell sorting (MACS). As conventional cytometers are both bulky and costly, there is a growing need to reduce the volume and cost of the fluidic and optical system. Consequently, many projects are focused on designing portable and even disposable microflow cytometers. The "flow cytometry on chip" section in Andersson and van den Berg's review [2] provides a very extensive summary of the research done in this field. As a complement to their review, we present additional studies including the latest publications on the same topic [11-24].

Detection methods for flow cytometry techniques can be either fluorescence or impedance based. Optical systems are well established in conventional cytometry, but there is a tendency for further integration with on-chip flow cytometer [11-16]. Lee et al recently designed and fabricated a micromachined flow cytometer integrated with buried SU-8/spin-on-glass optical waveguides [11], and then applied the same principle of optical detection to microcapillary electrophoresis chips for bioanalytical application [12]. Regarding integration of optical systems with a microchip, two other groups have made contributions [13, 14]. Morgan's group successfully developed a dielectrophoretic

lab-on chip with integrated particle detection [13], while Nieuwenhuis's group incorporated two elongated photodiodes on the bottom of the flow microchannel [14]. Lee's group reported on flow cytometer on chip with two embedded etched optic fibers enabling on-line detection of cells [15]. They used polished soda-lime glass substrates to fabricate the device and optical fibers glued to the etched fiber channels with UV-sensitive glue. By using three-dimensional hydrodynamic focusing (Fig.1), they successfully counted polystyrene beads and blood cells by recording the scattering signals, a method which does not require labeling. Their most recent study presents a microfabricated flow cytometer with integrated optical fibers, electrokinetic focusing and an electrokinetic flow-switch [16].

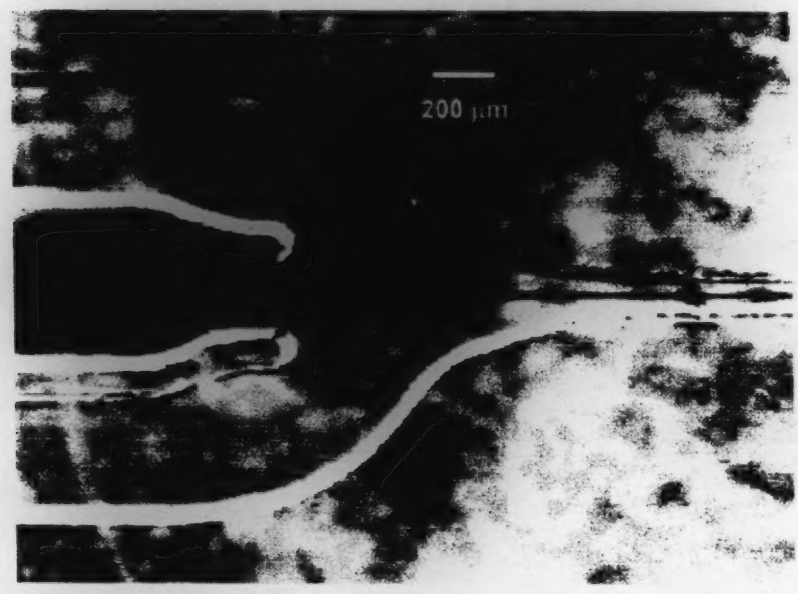

Figure 1-1. Hydrodynamic focusing effect of the micromachined flow cytometer. The width of the focused stream is 10 μm. (Adapted from reference 15)

Quake's group also presented a microfabricated cell sorter, using it for the separation of E.Coli cells expressing green fluorescent protein (GFP) from non-fluorescent E.Coli cells [17, 18]. In 1999, they used a disposable silicone elastomer chip and manipulated bacteria cells by electroosmotic flow [17]. Three years later, they demonstrated sorting and recovering of E.Coli once more, but this time they used a pressure driven cell sorter. The device had the same basic design as the microchip in their previous study, except that valves and pumps were incorporated [18]. Both devices were made from inexpensive material and could be disposable, eliminating the threat of possible cross-contamination from previous samples. The idea of a disposable microflow cytometer was also shown in the study in Takayama's group [19]. Their work was particularly interesting because they used air instead of liquids as a sheath fluid. In this way, they reduced the size of sheath liquid reservoirs, reducing the manufacturing cost as well as the volume and weight of the device. The chip was made from polydimethylsiloxane (PDMS) and its performance was tested by changing the flow rate and examining the surface chemistry of the channel walls. C_2C_{12} myoblast cells labeled with Syto 9 were successfully counted. In addition to all these studies, there are a few other interesting publications on flow cytometry on chip, which deal with different problems such as studying microrheology of erythrocytes, impedance based and dielectrophoresis (DEP) based flow microcytometers or cell sorting based on the intrinsic autofluorescence of living cells [20-23].

1.2.2 Monitoring of Cells in a Steady State

Much effort has gone into developing different techniques and tools for monitoring cell properties in a steady state. Light microscopy, video microscopy, calorimetry and impedance measurements are all well-known techniques used in cell population studies. Following the miniaturization trend, many of these techniques have successfully been transferred to microfluidic devices, which became an efficient and popular instrument for observing a variety of cell population features such as cell permeability, cell shape, cellular volume, cellular energy consumption or cellular impedance.

In 2000, Howard and Rubinsky [24] built a microdiffusion chamber that showed excellent results in determining the permeability of a cell membrane in various osmotic conditions. They used a human breast cell line (HBL-100 cells) to study the membrane permeability of trapped single cells. They demonstrated a feasible technique for studying kinetic volume changes when the media is continuously changed. Their data show the relative cell volume increasing when the trapped cell is exposed to glycerol and a volume drop when it is exposed to NaCl solution. This method has great importance for the field of cryobiology, because the kinetics of cell water and permeant transport has to be determined before designing any cryobiological procedure.

As shown earlier, cell shape and size have always been important in cell studies. Tracey et al. built and then improved a micromachined device for the measurement of cell volume index and flow velocity profile [25, 20]. Recently, Barakat and coworkers have developed a microfabricated platform in order to study relationships between endothelial cell (EC) shape and function [26]. They grew bovine aortic endothelial cells (BAECs) in microchannels under static culture conditions. The channel width varied from 25 to 225 μm. As their data show (Fig. 1-2), cells were oriented mostly along the channel length as the channel width decreased. If channels were wide, cells were oriented randomly. Another study was done by exposing EC to a steady shear stress of 20 dyne/cm^2, and the results showed that cells tend to elongate and align in the direction of flow. The results are in agreement with those obtained by three other research groups, who observed ECs exposed to shear stress when cultured on plain surfaces [27-29].

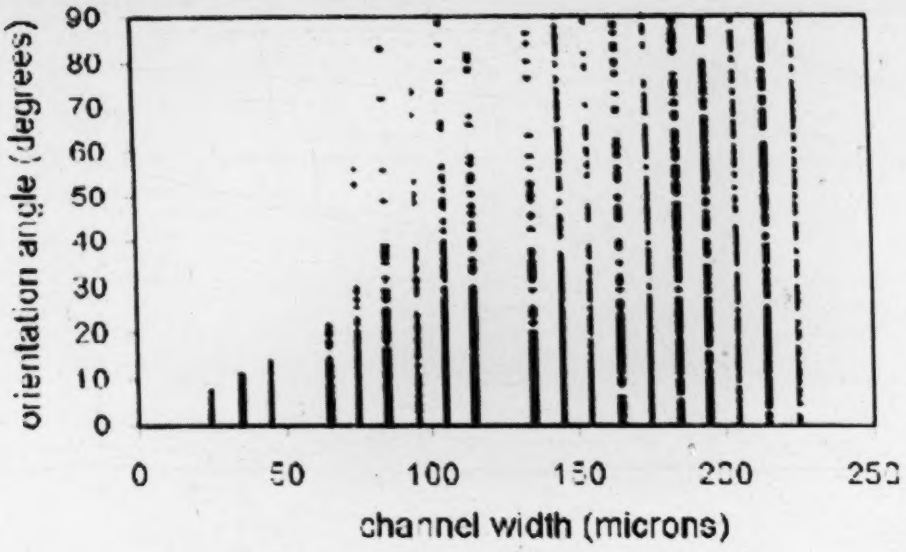

Figure 1-2. Orientation angle for BAECs cultured in microchannels as a function of microchannel width. The axis along the channel length is defined as zero degrees. The extent of cell alignment increases with channel width. (Adapted from reference 26)

Cellular energy consumption and genesis are excellent parameters for screening cellular metabolic activity. Whole cell sensors are becoming more popular in application to cell monitoring studies. In 1999, Verhaegen et al. [30] demonstrated calorimetry measurements of Xenopus Laevis cultured kidney cells on a micromachined silicon chip. These experiments demonstrated greater feasibility of this micromachined device over conventional microcalorimeters on the market, because they do not need to be complemented with an additional functional assay. While this device still focused on calorimetric measurements of a large cell number, three years later Cooper and coworkers [31] presented a microsystem sensor technology for cellular calorimetry that could provide information on single cell response. They stimulated isolated rat myocytes and mice brown adipocytes by carbonyle cyanide (m)- chlorophenyl hydrazone or norepinephrine to increase respiration and heat output. They recorded the response from 20 or 10 cells and the single cell response matched literature values.

Cell impedance studies have always been very helpful in a variety of research areas. For example, neuroscience has a great interest in neuronal electrical activity, because it offers very useful information when applied to pharmaceutical testing or biosensor research. In 2000, Wheeler et al. [32] showed that microelectrode arrays represent one of the most convenient tools for recording action potentials in vitro. They used embryonic hippocampal neurons patterned on a microelectrode array to create neural networks in serum-free culture. As the neuronal electric activity was exhibited for up to 29 days in vitro, they demonstrated that a microelectrode array can be used for the study of the dynamic behavior of neuronal networks. Two years later, Yasuda and coworkers [33] designed a microchamber system for neuronal cell cultivation equipped with electrodes for continuously following electrophysiological responses.

Impedance measurements could also be performed as a single cell screening method for cells in a continuous flow. Several researchers have used a flow cytometer on a chip, as it is an excellent instrument for impedance spectroscopy studies [21, 34-37]. In all those studies, opposing electroplated electrodes were placed in the micromachined channels through which cells were driven by pressure. Blood cells were used for all flow cytometry experiments, except the newest study where Frazier and coworkers [37] demonstrated impedance spectroscopy measurements on chromaffine cells. They have shown that this technique could be used as a cell identification method, because each cell type has its own impedance value. They successfully distinguished between chromaffine cells and erythrocytes, while Renaud et al. [35] were able to recognize erythrocytes and ghost erythrocytes (i.e. cytoplasm has been replaced by PBS) in the flowing stream and then separate them by dielectrophoresis. The most recent study of Renaud and coworkers [36] presents improvements of the device they used for previous experiments. They have used the same principle to discriminate and separate lymphocytes from granulocytes but their new device can also perform cell focusing and cell sorting, and it has improved the detection electrode geometry. They even made an experimental comparison of a cytometer/sorter on chip with a conventional FACS device, which discriminates cells according to forward and side scattering. The final results are quite similar, but on-chip electrical detection offers a big advantage because it is significantly less expensive.

Sometimes impedance measurements can even describe cellular and intracellular activities. Jager et al. [38] built a closable microvial for impedance recording that could provide information about cell spreading and aggregation of pigment granules within single cells.

Another interesting study used impedance measurements as a viability assay for bacterial cells extracted from food, soil or body fluids [39]. According to the reported data, there is a big difference in impedance measured in a suspension of bacteria compared with the impedance produced in a plain buffer. It is also important to note that impedance values increase as the concentration of bacteria increases (Fig. 1-3).

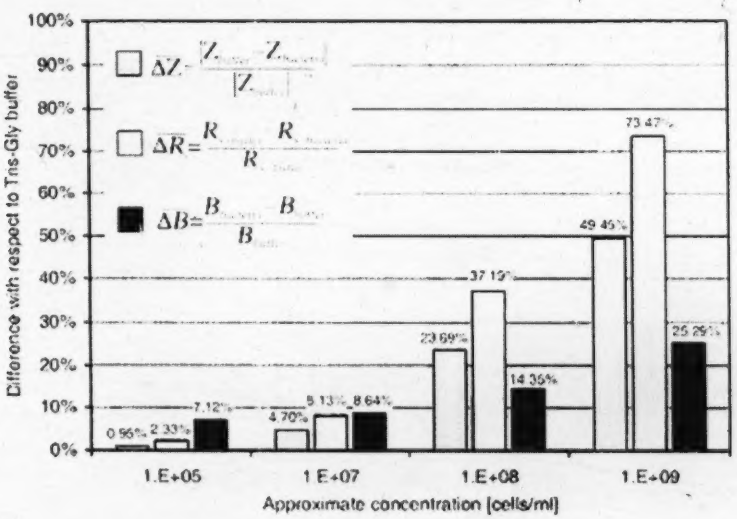

Figure 1-3. Normalized differences $\overline{\Delta Z}$, $\overline{\Delta R}$ and $\overline{\Delta B}$, for each concentration of L, innocua. (Adapted from reference 39)

Analysis of cell deformity in terms of shape, volume or membrane permeability has great importance in hematology, oncology, toxicology and environmental science. On the other hand, cellular energy activities as well as electric properties provide useful information for neuroscience and pharmaceutical tests. As a conclusion, these studies

give us good evidence that microchips will be further used and improved for monitoring different cell properties in a steady state.

1.2.3 Metabolic Monitoring

In order to monitor the kinetics of metabolism in a single cell, the metabolic process of interest has to be triggered by the appropriate stimulant. Once the process has started, it can be quantified by different bioassays, which may require cell lysis or could be performed on intact cells. In the following part of the review, we summarize the methods for cell lysis on chip as well as different techniques designed to follow specific reactions of cell metabolism. There is a focus on DNA and RNA studies that involve their on-chip isolation, single-cell enzymatic assays and research related to cell response manifested through hormone secretion.

Cell lysis on chip has become an attractive idea as research in developing microfluidic systems is shifting towards the subcellular level. In 1997, Li and Harrison [40] made preliminary steps towards cell metabolic monitoring on-chip that involves cell lysis. Using a voltage gradient, they introduced sodium dodecyl sulfate (SDS) into a microchannel and subsequently caused erythrocyte lysis in the mixing area of the microdevice. In this case, cell lysis happened due to disruption of the membrane, which was frequently used in many other on-chip studies [41-46]. Cell lysis can also be achieved by electrical degradation [47], heating [48] or a "freeze-thaw" technique [49, 50]. These lysis methods are specifically suitable for RNA isolation because they are gentle enough not to damage the components of the interest.

In 2001, Ramsey et al. [51, 52] studied different lysis techniques in order to find the best solution for rapid cell lysis on a microfluidic device. They used pressure driven Jurkat cells on a glass microfluidic device. They concluded that cell membrane disruption is most effective when chemical and electrical lysing techniques are combined. As their results show, this method is very convenient for microchip application because the lysing effects on chip are easily localized. As well, relevant cell components are well preserved, which is important for subsequent bioassays performed on chip. Yet it is significant that lysis happens very fast. Recently, the same research group published an

article, in which they achieved electrical cell lysis on chip in less than 33 ms [53], half the time they needed for an electrical-chemical lysis in a previous study [52]. Cell lysis as an element of complex procedures integrated on microfluidic devices should help in cell and molecular biology, genetics, biochemistry and many other branches of science.

As modern science is facing a rapidly increasing need for genetic information, microfluidics contributes by providing the tools for genetic analysis. One of the biggest challenges in this area is on-chip cell lysis integrated with subsequent analysis of RNA and DNA [43, 48, 49, 54-57]. In 1998, Ramsey and coworkers built a microchip for cell lysis, mutiplexed polymerase chain reaction (PCR) amplification and electrophoretic sizing [48]. Several years later, Nagai et al. [43] developed a high throughput single cell PCR process on chip. By using Jurkat cells, they presented a novel method for single cell isolation in a silicon micro chamber, followed by PCR analysis of the isolated cell genome. In 2003, Yeung and coworkers [49] did a project of similar character that enabled measurement of gene expression directly from single cells in a tiny capillary. In their experiments, they used a human lymphoblast cell line (GM13072), a human breast cancer cell line (T47D) and a human hepatoma cell line (HepG2). Although they integrated cell lysis, DNAase treatment, reverse transcription – PCR and CE with laser induced fluorescence (LIF) detection for gene expression, they still were not able to inject a single cell into a capillary, and the capillary itself was much longer than was necessary for the completion of the targeted RNA identification. In order to finalize the complex process consisting of so many steps, incorporation of an automated cell injection step as well as miniaturization of the device onto a chip must be achieved.

Collecting genetic information using microdevices has obviously become wide spread in research laboratories. There are many examples of the on-chip bioassays discussed above that employ cell lysis followed by the analysis of a cell genome. Beside these studies, there are many others reporting manipulation of already extracted DNA and RNA in microfluidic devices. This direction of research has opened up a whole new field with a current explosive expansion.

Metabolic monitoring of a cell undergoing lysis on chip does not focus only on the analysis of genetic material. A variety of research areas show great interest in

studying different cell components after they are released from the lysed cell. Those components are often cell enzymes, whole organelles or even single proteins, lipids and ions. Cell enzymes have an essential role in numerous biochemical paths that exist in each cell and many enzyme deficiencies cause severe diseases. In order to provide a tool for early diagnosis of the disease as well as a potential enzyme replacement therapy, it was useful to establish a high throughput single-cell enzymatic assay. In 1998, Harrison and coworkers [41] presented a microdevice for determining β-galactosidase activity from a single cell. They integrated on-chip lysis and incubation of a single promyelocytic leukemia cell (HL-60) with fluorescein-di-β-D-galactopyranoside (FDG) as well as fluorescence response detection. This new approach to the β-galactosidase screening offers advantages over the flow cytometry method that was previously widely used for this type of analysis. The on-chip technique eliminates the step of FDG uptake by intact cells, which was often variable, slow and low. Instead, lysed cells released β-galactosidase in a FDG rich medium, resulting in a 19 times higher fluorescence signal than viable cells incubated with 200 μM FDG. Three years later, Yager et al. [42] presented a similar study, which describes on-chip E.Coli lysis, and subsequent fluorescence detection of β-galactosidase released from the cell. The difference from Harrison's work was the design of the microdevice and fluorogenic substrate they used for enzyme detection (resorufin-β-D-galactopyranoside, RBG). The principle of the detection method remains the same, because the fluorogenic substrate is again cleaved by β-galactosidase resulting in release of the fluorophore. Besides β-galactosidase screening, many other enzyme assays have been performed on microfluidic devices. All of them predominantly use extracted enzymes at the very beginning of the on-chip process rather than whole cells.

As cell metabolism monitoring scales down to the subcellular level, microfluidic devices are being developed for cell organelle isolation and study. In 2001, Jensen et al. [44] lysed human HT-29 cells by applying an electric field and then used isoelectric focusing to direct released mitochondria towards their pI value. They created a pH gradient in the fluidic channel simply by applying an electric field and they further studied mitochondria electrophoretic mobility at different pH gradient values. A year

later, Kitamori and his collaborators [46] built a system for monitoring cytochrome c released from mitochondria to cytosol during apoptosis of NG 108-15 neuroblastoma-glioma hybrid cell. They did not perform rapid cell lysis, but they triggered the apoptosis process so they could monitor the changes within a single cell. Their system consisted of a scanning thermal lens microscope and microchip. The chip was designed to culture single cells first, and then start the process of apoptosis by introducing staurosporin. Active mitochondria in a cell were visible because they were stained by MitoTracker Green. The distribution of the cytochrome *c* was monitored due to the fact that it has a strong absorption around 532 nm. The whole principle offered the advantage of real time monitoring of the apoptosis process with respect to the cytochrome *c* redistribution profile.

In order to monitor metabolic processes, it is sometimes a requirement to preserve a whole cell. For example, Ca^{2+} flux is often studied because it is the key element in the process of signal transduction from the membrane to the cytoplasm. It can also be a part of the cell response to drug exposure. Andersson, Harrison and coworkers [58] have studied Ca^{2+} flux in a single human T and B lymphocyte using the stop-flow mode of microfluidic device. They examined the effect of two activator/inhibitor pairs: A23187/verapamyl and formyl-Met-Leu-Phe (f-MLP)/ mefenamic acid (MA). Another metabolic process studied in this paper was the oxidative burst in neutrophils. The process was quantified by a fluorescence indicator, which was previously loaded into neutrophils. The oxidative burst was triggered by phorbol myristate acetate and it resulted in three classes of the response due to several types of neutrophils. Recently, Daridon et al. [45] built a programmable cell assay platform that can be used as a "stand alone" system or integrated within a more complex system. They also performed a Ca^{2+} flux experiment using Jurkat T-cells loaded with a fluorescent indicator. The Ca^{2+} ionophore they used was ionomycin (Calbiochem) and the cell response was shown as fluorescence intensity vs. time. They have gone a step further toward Ca^{2+} flux monitoring in a single cell, introducing a physical isolation of a cell in a microchamber of the device.

Cell-based sensors are suitable for microfluidic devices. Cell properties related to cell communication with the external environment are used for detecting different agents

that will trigger a cell response. A change of color or fluorescence generation are most often used to signal the presence of the agent or of the reaction. There are a few studies of on chip, cell-based sensors. They are developed for allergen, glucose level and hormone detection.

There is a great need for rapid allergen detection tests because the methods currently used are time consuming. Matsubara et al. [59] fabricated a mast cell-based sensor on a PDMS chip for allergen detection. When stimulated by allergen, mast cells secrete histamine, which is released from the cell through the process of exocytosis. As the cells are previously loaded with quinacrine fluorescent dye, the dye is simultaneously released with histamine. Consequentially, the whole process is easily verified by fluorescence intensity recorded by a fluorescent microscope. Last year, another study was published reporting on the same topic [60]. In terms of the assay improvement, histamine was quantified more accurately because it was derivatized with o-phthaldehyde as soon as it was released from the mast cells. The PDMS microfluidic device had a more complex design compared with the previous study. It consisted of two units: a histamine release section and a fluorescence derivatizing section.

An on-chip glucose sensor used to study cell metabolism represents a very attractive project, with relevance to a variety of applications. There are two studies described employing on-chip glucose detection and monitoring single cell metabolism. One of them considers the metabolic reaction occurring in a living cell as an indicator of cell viability. This idea is used in a study presented by a group of scientists in 2001 [61]. They used the metabolic process in yeast cells that converts sucrose to glucose and ethanol as a proof of cell vital function. Yeast cells were immobilized on a silicon chip surface. After the addition of sucrose, glucose and ethanol were produced and subsequently oxidized, forming H_2O_2, which participated in a chemiluminescent reaction resulting in luminol. The luminol was detected by a photomultiplier. The enzymes for all the reactions were also co-immobilized on the chip surface.

The other study reports on a device that is also equipped with a glucose sensor, and has a great significance for research on human diabetes [62]. There are no details given about the sensor because it is used only as a tool for the monitoring of islet cell

function. The PDMS device is designed to trap single islet cells and to monitor hormone secretion. Recorded extracellular glucose levels provide information on insulin and glucagon secretion from the cell, which is the main feature of islet cell function. This is not the only project in the field of microfluidics that explores on-chip cell response to different stimuli manifested as hormone secretion. Tauseef et al. [63] used a human estrogen receptor (ER) of thyroid hormone receptor β (TRβ) engineered yeast cells to demonstrate on-chip detection of estrogen and thyroid hormone. The principle of detection was a color change of yeast cells, or a fluorescent product. This is a good example of a microfluidic device that successfully detects cell response initiated through cell receptors. Another study monitors the stimulation of cell receptors. Davidsson and coworkers [64] stimulated surface receptors of HeLa cells immobilized on a silicon microchip. They monitored receptor–mediated signal transduction using the reaction of luciferase and enhanced green protein formation.

Metabolic monitoring on chip provides us with a variety of information in a quick, cost effective way using a tiny volume of sample. Very often this is the best possible technique for insight into a single cell metabolic process. Different methods are developed for cell lysis, giving access to organelles, genetic material, enzymes, hormones and other biomolecules of clinical interest. From the aspect of using cells for the specific determination of different agents, microfluidic devices containing cell-based sensors have become wide spread tools in the pharmaceutical industry, contributing to new drug discoveries. These exciting results certainly encourage further development of microfluidic devices that will be implemented in clinical diagnostics.

1.2.4 Cell Based Drug Screening and Tumor Pathology On Chip

The demand for drug discovery screening technology has triggered a variety of different approaches to development in this area. The beginnings of cell based drug screening on chip monitor drug effects on cell metabolism. Nowadays, there is a strong effort for improving high throughput cell based drug screening that will maximally reduce analysis time and cost for both development and routine use of drug screening tests. It is also interesting to mention that many of these cell-based tests are focused

toward tumor pathology diagnostics. As is known, cancer initially starts with the disease of a single cell, progressing toward a metastatic disease that affects the whole body. From this reason, novel technologies and improved miniaturized devices that would assess cancer disease in its early stage are needed to enable the successful treatment and recovery of the patient.

Ca flux in a single cell is a significant indicator of the following cell activity. That is why this metabolic process often represents a favorable monitoring event. In 1997, Harrison et al. [58] presented a study examining Ca^{++} flux in a single lymphocyte. We have already introduced this paper from the aspect of metabolic monitoring but it is important to say that this on-chip bioassay also represents the drug screening method. They used verapamyl and mephenamic acid for inhibiting A23187 and formyl-Met-Leu-Phe ionophores. A potential new drug could be tested in this way to verify its ability to activate or inhibit Ca^{++} transport into the cell. A step further toward drug screening on chip was made in 1998 [65], when the same group of researchers presented a microfluidic device for the screening of anti-inflammatory drug candidates. They used the initial step of the inflammatory cell response; cell rolling, to test the anti-inflammatory effect of the following drugs: anti P-selectin, anti E- selectin, sialyl lewis and fucoidan. One side of the channel was coated by the drug of interest (inhibition side, A), while the other one (rolling side, B) was left uncoated providing an internal control. Rolling capabilities of the different cell types were tested: human blood cells, Jurkat cells or HL-60. This kind of test could further improve the procedure for examining new drugs in terms of reduced time and cost.

It seems that these two studies were a very successful beginning of an expansion of the microfluidics area in the direction of cell based drug screening. The latest projects are developing microdevices for high-throughput cell based drug screening. Yun et al. designed a nano-fluidic chip that enables nano-liter drug injection for single–cell analysis [66]. Cooper and coworkers [67] presented a high density array of assay sites for cell-based drug profiling. Using light microscopy, they recorded cell shortening and intracellular calcium of an individual heart muscle cell. The conditions in the microdevice

provided a comparison of the cells in normal and ischemic environments, giving an excellent cell-based model for testing potential therapeutic agents for heart failure.

Another throughput drug screening microsystem was designed by Oka et al. [68]. They tested the electrophysiological response of ganglion cells treated by glutamate. Their results suggest that the devices they fabricated successfully detected an excitatory effect of glutamine on ganglion cells. Future work may be done to improve the sensitivity of the device in order for it to be used in routine drug screening procedures.

Anti-cancer drugs have always been of great interest. Microfluidics has made its own contribution to this field, developing microarray cell based chips for high throughput screening of potential anticancer drugs. Tamia et al. [69] used HeLa229 cells for testing the cytotoxic activity of the carotenoids and carotenoid chemicals isolated from bacterial cultures. They monitored the cytotoxic activity of the above-mentioned substances by fluorogenic substrate-calcein. A fluorescence intensity drop was related to cancer cell death, i.e. anticancer activity of the examined drug.

In the area of tumor pathology, one of the main goals is to improve old methods and find new ones to distinguish normal from malignant cells. In 1995, it was shown that cancer cells can be separated from erythrocytes and T lymphocytes on the basis of their different dielectric properties [70]. The authors of this study performed the separation in a dielectric affinity column containing a microelectrode array. Their results demonstrate a significant difference between the dielectric properties of the cancer cells and normal blood cells. Four years later, very interesting work was done by Gourley and coworkers [71], who presented a completely different approach to the differential identification of healthy and cancer cells. They created a nanolaser/microfluidic biochip for distinguishing these cells using a total cell protein assay. For the first time, a microfluidic flow of cells was incorporated inside a microcavity laser, enabling the screening of cells in their native state. An intracavity spectroscopy technique was successfully employed to provide information on the protein concentration in the cells. The authors also recorded emission spectra of normal human astrocytes and glioblastoma cells (the most dangerous type of malignant astrocytomas) using a static biological microcavity laser. Results show

differences in spectral positions of the cell resonances (Fig.6), which could be used as a distinguishing label between those two cell populations.

The future brings an even stronger tendency for more intensive application of these devices both in laboratory routine and research protocols. Further miniaturization of chemical and biochemical analyzers will provide us with personal, portable analyzers that will be cost–effective and user-friendly. The trend towards inexpensive disposable devices of different designs, pushed by commercialization, will bring another benefit for medical institutions, industry and research laboratories. The future prospects of microfluidics certainly include more sophisticated devices that would be able to perform numerous cell analyses with shorter analysis time, higher sensitivity and lower cost.

1.3 Mitochondria and Apoptosis

1.3.1 Mitochondria

A mitochondrion is an oval shaped organelle about 0.5 μm in diameter and 1 μm in length. It has a smooth outer membrane, while the inner membrane has many invaginations (cristae). The number of these invaginations depends on respiratory activity of the cell type, because proteins involved in electron transport and oxidative phosphorylation are bound in the inner mitochondrial membrane. In the inner mitochondrial compartment, there is a gel-like substance, which is called the "matrix", containing soluble enzymes of oxidative metabolism, genetic material (DNA, RNA, ribosomes), nucleotide cofactors, substrates and inorganic ions. Mitochondria, which are highly heterogeneous within a cell [72-74] have important cellular functions such as electron transport and oxidative phosphorylation [75]. They also have a significant role in the apoptosis process [76, 77, 72] and in Ca^{++} homeostasis, while their malfunction is related to different diseases [78]. The mitochondria membrane potential, $\Delta\psi_M$, is a good indicator of mitochondria dysfunction because it changes whenever the mitochondria are damaged. $\Delta\psi_M$ of healthy mitochondria is established and maintained at about 180-220

mV by a complex mechanism, which includes the integrity of mitochondrial structure, electron transfer redox centers for oxidative phosphorylation, catalytic integrity of enzymes in β-oxidation and the Kreb's cycle and other transport mechanisms that connect the mitochondrial interior with the cytosol [79]. Thus, after it is determined that $\Delta\psi_M$ has changed, it may not be possible to assess the etiology of the mitochondria malfunction due to the complexity of the generation of the $\Delta\psi_M$.

1.3.2 The Role of Mitochondria in Apoptosis

The word "apoptosis" comes from a Greek word, "falling off", and science uses it to describe the process of programmed cell death. Together with cell proliferation, it is a mechanism that provides homeostasis of all tissues. The complex process of apoptosis involves a series of events, which includes different morphological changes such as DNA fragmentation, cell shrinkage, protein degradation and alterations in mitochondria activities and membrane potential ($\Delta\psi_M$). The apoptosis process could happen through two major pathways: extrinsic and intrinsic. The extrinsic pathway happens through the cell "death" receptors such as the tumor necrosis factor (TNF) receptor, Fas, or the tumor necrosis factor–related apoptosis inducing ligand (TRAIL), while the intrinsic pathway involves mitochondria. There is a strong trend to study all the details regarding the apoptosis process, because each of these steps potentially represents a tool for apoptosis regulation. For example, Yagami and coworkers focused on the regulation of DNA fragmentation and chromatin condensation using anti-inflammatory drugs [80]. Other research groups studied biochemical changes, which involve the activity of caspase enzymes [81,82] regardless of the apoptosis pathway. Susin et al. demonstrated that a $\Delta\psi_M$ drop is one of the first events of a cell undergoing apoptosis [83]. They examined a variety of cell models and, each time, $\Delta\psi_M$ was reduced before any appearance of apoptotic nuclear changes. This is certainly the reason that apoptosis studies focus on mitochondria activities and changes in $\Delta\psi_M$ as the most crucial apoptosis indicators [81-88]. During the apoptosis process, mitochondria express changes in electron transport and oxidative phosphorylation function. In addition to that, they release apoptosis – stimulating compounds such as cytochrome *c*, apoptotic inducing factor (AIF) and

procaspases. Another important element is a drop in $\Delta\psi_M$, which is present regardless of the agent used to trigger the apoptosis process (valinomycin, Concavalin A, staurosporine, rotenon or any other agent). The mechanism of affecting $\Delta\psi_M$ is always related to alterations in the permeability of the mitochondria membrane. For example, in our experiments apoptosis is triggered by valinomycin and oligomycin. The former transfers K^+ ions through the mitochondrial membrane and the latter blocks the activity of mitochondrial ATP-ase (F_o), both resulting in reduced $\Delta\psi_M$.

1.4 Overview of the Methods Used to Characterize Mitochondria Properties

Many techniques have been used in studying different mitochondria properties such as $\Delta\psi_M$, Ca^{++} concentration and uptake, membrane structure, permeability transition, mitochondria permeability transition pore, electrophoretic mobility, etc. Microscopy techniques for *in situ* measurements, flow cytometry, capillary electrophoresis, patch-clamping and optical trapping have been widely used for examining individual mitochondria. Recently, Fuller and Arriaga have published a review that summarizes a large number of papers describing all the different methods employed in mitochondria analysis [89]. In addition to all these techniques, we mention mitochondria analysis using microfluidic devices, which is rapidly gaining popularity [50, 23, 90].

As $\Delta\psi_M$ was monitored in nearly all our experiments, this section provides more details on the different techniques and potentiometric dyes that are commonly used for $\Delta\psi_M$ assessment. The principle is basically the same for all dyes: positively charged, lipophylic molecules diffuse into cells and then into the mitochondrial matrix due to the potential difference. Under ideal conditions, with no interference by binding to other cellular components or by transport by other carriers, molecules of the dye will achieve equilibrium due to the electrochemical gradient. At that point, the potential difference across the membrane is easily calculated by the Nernst equation, knowing the dye concentrations on both sides of the membrane. In the past, radioactive Rb and

radiolabeled tetraphenylphosphonium ion (TPP^+), were used to measure $\Delta\psi_M$. There is another technique, which is still used for real-time kinetic measurement of mitochondria membrane potential, and it involves a TPP^+ electrode. Basically, TPP^+ concentration at the outer mitochondrial space is monitored. If the TPP^+ concentration is decreased, there is hyperpolarization present and vice versa. Nowadays, monitoring of $\Delta\psi_M$ is usually done with commercially available fluorescent, lipophylic, cationic dyes: JC-1 (5, 5', 6, 6'-tetrachloro- 1, 1', 3, 3' tetraethylbenzimidazolyl-carbocyanine iodide), rhodamine 123, TMR (tetramethylrhodamine) and $DiOC_6$ (3,3'- dihexyloxacarbocyanine iodide). There is an assumption made that dye uptake is proportional to the membrane potential, which is applicable to all the above listed fluorescent dyes except JC-1. JC-1 stain is a ratiometric indicator of $\Delta\psi_M$, where the red/green fluorescence ratio for an undamaged $\Delta\psi_M$ is higher than the ratio of a damaged $\Delta\psi_M$. Red fluorescence comes from the dye molecule aggregates located at the membrane of undamaged potential, while green fluorescence comes from the dye monomers, which are present at membranes with damaged potential. More details about JC-1 are described later in Section 2.2.2. of Chapter 2. Comparing all the fluorescent dyes, JC-1 appears to have advantages over the other three because it is mitochondria selective, which is not the case with the others [91, 79]. On the other hand, the JC-1 stain needs a more complex detection system in order to obtain interpretable data. In the experiments for monitoring $\Delta\psi_M$, measurements of the fluorescence are usually done by fluorescence microscopy or flow cytometry, which provide real-time fluorescence changes or fluorescence at one time point, respectively.

1.5 Monitoring Mitochondria Membrane Potential as a Tool in Drug Trials

In order to study and better understand each step of the apoptosis process, it is necessary to use an agent that will trigger a series of cell events leading toward programmed cell death. The regulation of this process is extremely important both when apoptosis is to be inhibited and promoted.

In the case of chemotherapy, apoptosis-resistant malignant cells represent a great problem because most of the chemotherapeutic agents act through cell programmed death. This is the reason that many research groups have carefully studied the drug resistance of a variety of malignant cells. Two research groups studied apoptosis-resistant phenotype in leukemia cells [92, 93]. The results show that synthesis of Bc1-2 protein at the outer mitochondrial membrane may be responsible for the resistance expressed toward anthracycline treatment. The other group characterized the drug resistant mechanism in acute myeloid leukemia, showing the key role of the P-glycoprotein (Pgp) [93].

Other research groups carefully studied the mechanism of apoptosis in tumor diseases, providing a great contribution to understanding apoptosis regulation and to drug development. Rabinowich and coworkers examined an inhibition of the FAS receptor and extrinsic (mitochondria) pathway in Jurkat leukemic T cells [94, 95]. Mancini at al. studied delayed apoptosis in a human colon carcinoma cell line induced by herbimycin A [96]. They observed unrestrained mitochondrial proliferation and progressive membrane dysfunction as a part of the apoptosis mechanism in these cells. Hirpara's research group demonstrated the significance of hydrogen peroxide production in the apoptosis process [97]. In addition to many other studies, we also mention Chow and coworkers, who presented a very interesting in vitro study of Hodgin's lymphoma cells treated by established cytotoxic drugs and bendamustine. They demonstrated the importance of drug interaction aspects, which sometimes can result in the failure of the treatment because of the antagonistic effects between the two drugs.

Apoptosis is not only studied in relation to tumor diseases. Many research groups investigated the significance of apoptosis in HIV infection [98-101]. For example, Cossarizza and coworkers investigated mitochondria alterations in peripheral blood lymphocytes during acute HIV syndrome [101]. $\Delta\psi_M$ was also monitored in examinations of antimalaric drugs. Srivastava and collaborators have demonstrated that the broad-spectrum antiparasitic drug, atovaquone, depolarizes malarial mitochondria with consequent cellular damage and death [102].

1.6 Scope of the Thesis

The goal of the thesis is focused on the design and testing of a microfluidic chip with a multi-wavelength detection system for the analysis of cellular and subcellular devices, and then its comparison to flow cytometry methods.

In the second chapter, a preliminary experimental study is presented, along with a detailed discussion of the chemical stains, mitochondrial isolation methods and the procedures used to evaluate the mitochondria. The design and testing of a multi-wavelength detection system and the software needed for monitoring $\Delta\psi_M$ by JC-1 staining is described. Details of the protocol used to isolate mitochondria from Jurkat cells are given, along with the evaluation methods. Several simple fluidic studies of cells and mitochondria used to test the system are described as well.

Chapter 3 discusses the use of the chip-based flow cytometry system described in Chapter 2, employing a study of the effects of oligomycin and valinomycin on mitochondria in Jurkat cells, and isolated mitochondria. These drugs were used to trigger apoptosis, causing a change in $\Delta\psi_M$ that was monitored with fluorescence detection. Results are presented for studies of dose and time response of mitochondria to treatment with valinomycin and oligomycin. The results obtained on-chip were compared to studies performed by flow cytometry, in order to evaluate the chip performance.

In the final chapter, a brief summary of the achievements presented in the thesis as well as some suggestions for future work is made.

1.7 Bibliography

1. Krishnan M, Namasivayam V, Lin R, Pal R and Burns MA; Microfabricated Reaction and Separation Systems, *Current Opinion in Biotechnology* **2001**, 12:92-98
2. Andersson H, Van Den Berg A; Microfluidic Devices for Cellomics: a Review, *Sensors and Actuators B* **2003**, 92: 315-325
3. Sundberg SA; High-Throughput and Ultra-High-Throughput Screening: Solution and Cell-Based Approaches, *Current Opinion in Biotechnology* **2000**, 11:47-53
4. Burbaum JJ; Miniaturization technologies in HTS: How Fast, How Small, How Soon, *Drug Discovery Today* **1998**, 3(7): 313-349
5. Sunberg SA, Chow A, Nikiforov T and Wada HG; Microchip-Based Systems for Target Validation and HTS, *Drug Discovery Today* **2000**, 5(12): S92-S103
6. Paez X and Hernandez L; Biomedical Applications of Capillary Electrophoresis with Laser-Induced Fluorescence Detection, *Biopharmaceutics & Drug Disposition* **2001**, 22: 273-289
7. Dolnik V, Liu S and Jovanovich S; Capillary Electrophoresis on Microchip, *Electrophoresis* **2000**, 21:41-54
8. Bruin GJ; Recent Developments in Electrokinetically Driven Analysis on Microfabricated Devices, *Electrophoresis* **2000**, 21: 3931-3951
9. Dovichi NJ and Hu S; Chemical Cytometry, *Current Opinion in Chemical Biology* **2003**, 7:1-6
10. Krylov SN, Starke DA, Arriaga EA, Zhang Z, Chan NWC, Palcic MM and Dovichi NJ; Instrumentation for Chemical Cytometry, *Anal Chem* **2000**, 72: 872-877
11. Lee GB, Lin CH and Chang GL; Micro Flow Cytometers with Buried SU-8/SOG Optical Waveguides, *Sensors and Actuators A* **2003**, 103: 165-170
12. Lee GB, Lin CH, Chen SH and Chang GL; Microcapillary Electrophoresis Chips Integrated with Buried SU-8/SOG Optical Waveguides for Bio-Analytical Applications, *Sensors and Actuators A* **2003**, 107: 125-131
13. Cui L, Zhang T and Morgan H; Optical Particle Detection Integrated in a Dielectrophoretic Lab-On-Chip, *J Micromech Microeng* **2002**, 12: 7-12

14. Nieuwenhuis JH, Bastemeijer J, Sarro PM and Vellekoop MJ; First Measurement Results with an Integrated Projection Cytometer, *microTAS* **2003**, 2:1219-1222
15. Lin CH and Lee GB; Micromachined Flow Cytometers with Embedded Etched Optic Fibers for Optical Detection, *J Micromech Microeng* **2003**, 13: 447-453
16. Lee GB, Fu LM, Yang RJ and Pan YJ; Micro Flow Cytometers Using Electrokinetic Forces with Integrated Optical Fibers for On-Line Cell/Particle Counting and Sorting, *microTAS* **2003**, 1: 45-48
17. Fu AY, Spence C, Scherer A, Arnold FH and Quake SR; A Microfabricated Fluorescence-Activated Cell Sorter, *Nature Biotechnology* **1999**, 17: 1109-1111
18. Fu AY, Chou HP, Spence C, Arnold FH and Quake SR; *Anal Chem* **2002**, 74: 2451-2457
19. Huh D, Tung YC, Wei HH, Grotberg JB, Skerlos SJ, Kurabayashi K and Takayama S; Use of Air-Liquid Two-Phase Flow in Hydrophobic Microfluidic Channels for Disposable Flow Cytometers, *Biomedical Microdevices* **2002**, 4(2): 141-149
20. Sutton N, Tracey MC, Johnston ID, Greenaway RS and Rampling MW; A Novel Instrument for Studying the Flow Behaviour of Erythrocytes through Microchannels Simulating Human Blood Capillaries, *Microvascular Research* **1997**, 53: 272-281
21. Holmes D and Morgan H; Impendance Based Single Cell Detection Using Resonance Frequency Interrogation, *microTAS* **2003**, 2: 1239-1242
22. Vykoukal J, Schwartz JA and Gascoyne RC; Dielectrophoresis Based Micro Flow Cytometry, *microTAS* **2003**, 2: 1153-56
23. Emmelkamp J, Costa RD, Andersson H and van den Berg A; Intrinsic Autofluorescence of Single Living Cells for Label-Free Cell Sorting in a Microfluidic System, *microTAS* **2003**, 1:85-88
24. Howard KP and Rubinsky B; An Analysis of Unicellular Mass Tranfer Using a Microfabricated Experimental Technique, Biomedical Microdevices 2000, 2(4): 305-316
25. Tracey M, Greenaway RS, Das A, Kaye PH and Barnes AJ; A Silicon Micromachined Device for Use in Blood Cell Deformability Studies, *IEEE Transactions on Biomedical Engineering* **1995**, 42 (8): 751-761

26. Gray BL, Lieu DK, Collins SD, Smith RL and Barakat AI; Microcahnnel Platform for the Study of Endothelial Cell Shape and Function, *Biomedical Microdevices* **2002**, 4(1): 9-16
27. Dewey CF Jr, Bussolari MA, Gimbrone MA Jr and Davis PF; *Journal of Biomechanical Engineering* **1981**, 103:177
28. Nerem RM, Levesque MJ and Cornhill JF; *Journal of Biomechanical Engineering* **1981**, 103:172
29. Wechezak AR, Viggers RF and Sauvage LR; Laboratory Investigation 1985, 53: 639
30. Verhaegen K, Simaels J, Van Drieessche W, Baert K, Sansen W, Puers B, Hermans L and Mertens R; A Biomedical Microphysiometer, *Biomedical Microdevices* **1999**, 2(2): 93-98
31. Johannessen EA, Weaver JMR, Bourova L, Svoboda P, Cobbold PH and Cooper JM; Micromachined Nanocalorimetric Sensor for Ultra-Low-Volume Cell-Based-Assays, *Anal Chem* **2002**, 74:2190-2197
32. Chang JC, Brewer GJ and Wheeler BC; Microelectrode Array Recordings of Patterned Hippocampal Neurons for Four Weeks, *Biomedical Microdevices* **2000**, 2(4): 245-253
33. Takashi K, Sugio Yoshiro, Moriguchi H, Jimbo Y and Yasuda K; On-Chip Neural Cell-Cultivation System for Long-Term Observation with Multi-Electrode and Microchamber Arrays, *microTAS* **2002**, 841-843
34. Fuller CK, Hamilton J, Ackler H, Krulevitch P, Boser B, Eldredge A, Becker F, Yang J and Gascoyne P; Microfabricated Multi-Frequency Particle Impendance Characterization System, *microTAS* **2000**, 265-268
35. Gawad S, Metz S, Schild L and Renaud P; Impendance Spectroscopy Cell, *microTAS* **2001**, 253
36. Gawad S, Batard P, Seger U, Metz S and Renaud P; Leukocytes Discrimination by impendance Spectroscopy Flow Cytometry, *microTAS* **2002**, 649-651
37. Mohanty SK, Ravula SK, Engisch K and Frazier B; Single Cell Analysis of Bovine Chromaffin Cells Using Micro Electrical Impendance Spectroscopy, *microTAS* **2002**, 838-840

38. Jager EWH, Immerstrand C, Holmgren Peterson K, Mgnusson KE, Lundstrom I and Inganas O; The Cell Clinic: Closable Microvials for Single Cell Studies, *Biomedical Microdevices* **2002**, 4(3): 177-187
39. Gomez R and Bashir R; Microfluidic Biochip for Impendance Spectroscopy of Biological Species, *Biomedical Microdevices* **2001**, 3(3): 201-209
40. Li P and Harrison DJ, Transport, Manipulation, and Reaction of Biological Cells On-Chip Using Electrokinetic Effects; *Anal Chem* **1997**, 69, 1564-1568
41. Ocvirk G, Salimi-Moosavi H, Szarka RJ, Arriaga E, Andersson PE, Smith R, Dovichi NJ and Harrison DJ; Single Cell Enzymatic Analysis on Microchip: Lysing of Single Cells and Identification of Their β- Galactosidase Activity, *microTAS* **1998**, 203-206
42. Schilling EA, Kamholz AE and Yager P; Cell Lysis and Protein Extraction in a Microfluidic Device with Detection by a Fluorogenic Enzyme Asay, *Anal Chem* **2002**, 74:1798-1804
43. Nagai H, Murakami Y, Morita Y, Yokoyama K and Tamiya E; Development of Microchamber Array for Picoliter PCR, *Anal Chem* **2001**, 73:1043-1047
44. Lu H, Jackman RJ, Gaudet S, Cardone M, Schmidt MA and Jensen KF; Microfluidic Devices for Cell Lysis and Isolation of Organelles, *microTAS* **2001**, 297-298
45. Daridon A, Throndset W, Liau I, Farrell K, Tseng F, Javadi S and Manger I; A Programmable Cell Assay Platform for Kinetic Studies of a Single Cell, *microTAS* **2002**, 31-33
46. Tamaki E, Sato K, Tokeshi M, Sato K, Aihara M and Kitamori T; Single-Cell Analysis by Scanning Thermal Lens Microscope with a Microchip: Direct Monitoring of Cytochrome c Distribution during Apoptosis Process, *Anal Chem* **2002**, 74: 1560-1564
47. Kim MS, Lee SH, Cho SH, Lee CS, Kim BG and Kim YK; Electrolysis of Cancer Cells Using Isoosmotic Buffer Solution, *microTAS* **2001**, 293-294
48. Watters LC, Jacobson SC, Kroutchinina N, Khandurina J, Foote RS and Ramsey JM; Microchip Device for Cell Lysis, Multiplex PCR Amplification, and Electrophoretic Sizing, *Anal Chem 1998*, 70: 158-162

49. Matsunaga H, Anazawa T and Yeung ES; Integrated On-Capillary Instrumentation for Gene Expression Measurements Directly from Cells, *Electrophoresis* **2003**, 24:458-465

50. Zabzdyr JL, Lillard SJ; Measurement of Single-Cell Gene Expression Using Capillary Electrophoresis, *Anal Chem* **2001**, 73: 5771-5775

51. McClain MA, Culbertson CT, Jacobson SC and Ramsey JM; Single Cell Lysis on Microfluidic Devices, *microTAS* **2001**, 301-302

52. Culbertson CT, Alarie JP, McClain MA, Jacobson SC and Ramsey JM; Rapid Cellular Assays on Microfabricated Fluidic Devices, *microTAS* **2001**, 285-286

53. McClain MA, Culbertson CT, Jacobson SC, Allbritton NL, Sims CE and Ramsey JM; Microfluidic Devices for the High-Throughput Chemical Analysis of Cells, *Anal Chem* **2003**, ASAP article

54. Crabtree HJ, Bay SJ, Lewis DF, Zhang J, Coulson LD, Fitzpatrick GA. Delinger SL, Harrison DJ and Dovichi NJ; Construction and Evaluation of Capillary Array DNA Sequencer Based on a Micromachined Sheath-Flow Cuvette, *Electrophoresis* **2000**, 21(7): 1329-1335

55. Wilding P, Kricka LJ, Cheng J, Hvichia G, Shoffner MA and Fortina P; Integrated Cell Isolation and Polymerase Chain Reaction Analysis Using Silicon Microfilter Chambers, *Analytical Biochemistry* **1998**, 257: 95-100

56. Ronai Z, Barta C, Sasvari-Szekely M and Guttman A; DNA Analysis on Electrophoretic Microchips: Effect of Operational Variables, *Electrophoresis* **2001**, 22: 294-299

57. Yen PK, Kricka LJ, Fortina P, Panaro NJ, Sakazume T and Wilding P; Microchip Module for Blood Sample Preparation and Nucleic Acid Amplification Reactions, *Genome Research* **2001**, 11: 405-412

58. Andersson PE, Li PCH, Smith R, Szarka RJ and Harrison DJ; Technical Digest: 1997, International Conference on Solid State Sensors and Actuators, *Transducers* **1997**, June 16-19, 1331

59. Matsubara Y, Murakami Y, Kinpara T, Morita Y, Yokoyama K and Tamiya E; Allergy Based Sensor Using Animal Cells with Microfluidics, *microTAS* **2001**, 299-230

60. Tokuyama T, Fujii SI, Abo M and Okubo A; Cellular Analysis System of Histamine Release on Microchip, *microTAS* **2002**, 832-834

61. Davidsson R, Bengtsson M, Johansson B, Passoth V, laurel T and Emneus J; A Micro Total Analysis System for Monitoring Immobilized Yeast Cells Using an Enzymatic Chemiluminiscent Detection System, *microTAS* **2001**, 287-288

62. Gao C, Rilo HLR, Choi JW and Ahn CH; A Mirofluidic Biosystem for Metabolic monitoring of Human Islet Cells with Integrated Biosensors, *microTAS* **2002**, 787-789

63. Butt T, Tran H, Choi JW, Cho HJ and Ahn CH; A Disposable Cell-Based Biochip for Detection on Hormones and Drugs, *microTAS* **2001**, 83-84

64. Davidsson R, Bristulf J, Kotarsky K, Olde B, Owman C, Bengtsson M, Laurell T and Emneus J; Monitoring of Human Chemiluminescent Reporter Cell Lines Expressing G-Protein-Coupled Receptors in a Microfluidic System, *microTAS* **2002**, 811-813

65. Salimi-Moosavi H, Szarka R, Andersson P, Smith R and Harrison DJ; Biology Lab-On-Chip for Drug Screening, *microTAS* **1998**, 69-72

66. Yun KS, Lee SI, Lee GM and Yoon E; Design and Fabrication of Micro/Nano-Fluidic Chip Performing Single-Cell Positioning and Nanoliter Drug Injection for Single-Cell Analysis, *microTAS* **2002**, 652-654

67. Klauke N, Smith G and Cooper J; Microsystems technology for Cell Screening in New Medicines Discovery, *microTAS* **2002**, 853-855

68. Ozaki N, Ogawa R, Sugihara H, Emoto F, Tanabe M, Konishi S and Oka H; Electrophysiological High Throughput Drug Screening System, *microTAS* **2002**, 856-858

69. Rao SR, Akagi Y, Morita Y and Tamiya E; High-Throughput Screening of Anticancer Drugs Using Microarray Based Cell Chip, *microTAS* **2002**, 862-864

70. Becker FF, Wang XB, Huang Y, Pethig R, Vykoukal J and Gascoyne PRC; Separation of Human Breast Cancer Cells from Blood by Differential Dielectric Affinity, *Proc. Natl. Acad. Sci. USA* **1995**, 92:860-864

71. Gourley PL, McDonald AE, Hendricks JK, Copeland GC, Hunter J, Akhil O and Dunne JL, NanoLaser/Microfluidic Biochip for Realtime Tumor Pathology, *Biomedical Microdevices* **1999**, 2(2): 111-122

72. Krysko, D., et al., Mitochondrial Transmembrane Potential Changes Support the Concept of Mitochondrial Heterogeneity during Apoptosis. *The Journal of Histochemistry & Cytochemistry*, **2001**. 49 (10): p. 1277-1284.

73. Collins, T., et al., Mitochondria are Morphologically and Functionally Heterogeneous within Cells. *The EMBO Journal*, **2002**. 21 (7): p. 1616-1627.

74. Cossariza, A., D. Ceccarelli, and A. Masini, Functional Heterogeneity of an Isolated Mitochondria Population Revealed by Cytofluorimetric Analysis at the Single Organelle Level. *Experimental Cell Research*, **1996**. 222: p. 84-94.

75. Saraste, M., Oxidative Phosphorylation at the fin de siecle. *Science*, **1999**. 283: p. 1488-1493.

76. Rasola, A. and M. Geuna, A Flow Cytometry Assay Simultaneously Detects Independent Apoptotic Parameters. *Cytometry*, **2001**. 45: p. 151-157.

77. Cossariza, A., et al., Mitochondrial Modifications during Rat Thymocyte Apoptosis: A Study at the Single Cell Level. *Experimental Cell Research*, **1994**. 214: p. 323-330.

78. Wallace, D., Mitochondrial Diseases in Man and Mouse. *Science*, **1999**. 283: p. 1482-1488.

79. Pon, L. and E. Schon, Mitochondria. *Methods in Cell Biology*, **2001**. 65.

80. Yagami, T., et al., Effects of S-2474, a Novel Nonsteroidal Anti-inflammatory drug, on Amyloid b protein-induced neuronal cell death. *British Journal of Pharmacology*, **2001**. 134: p. 673-681

81. Bortner, C. and J. Cidlowski, Caspase Independent/Dependent Regulation of K+, Cell Shrinkage, and Mitochondrial Membrane Potential during Lymphocyte Apoptosis. *The Journal of Biological Chemistry*, **1999**. 274 (31): p. 21953-21962.

82. Follstad, B., D. Wang, and Stephanopoulos, Mitochondrial Membrane Potential Differentiates Cells Resistant to Apoptosis in Hybridoma Cultures. *European Journal of Biochemistry*, **2000**. 267: p. 6534-6540

83. Susin, S., N. Zamzani, and G. Kroemer, The Cell Biology of Apoptosis: Evidence for the Implication of Mitochondria. *Apoptosis*, **1996**. 1: p. 231-242.

84. Wadia, J., et al., Mitochondrial Membrane Potential and Nuclear Changes in Apoptosis Caused by Serum and Nerve Growth Factor Withdrawal: Time Course and Modification by (-)-Deprenyl. *The Journal of Neuroscience*, **1998**. 18(3): p. 932-947.

85. White, R. and I. Reynolds, Mitochondrial Depolarization in Glutamate-Stimulated Neurons: An Early Signal Specific to Excitotoxin Exposure. *The Journal of Neuroscience*, **1996**. 16 (18): p. 5688-5697.

86. Ludovico, P., F. Sansonetty, and M. Corte-Real, Assesment of Mitochondrial Membrane Potential in Yeast Cell Populations by Flow Cytometry. *Microbiology*, **2001**. 147: p. 3335-3343

87. Kulkarni, G., et al., Role of Mitochondrial Membrane Potential in Concavalin A-Induced Apoptosis in Human Fibroblasts. *Experimental Cell Research*, **1998**. 245: p. 170-178.

88. Kahlert, S., L. Schild, and G. Reiser, Mitohocndrial Polarization in Rat Hippocampal Astrocytes is Resistant to Cytosolic Ca^{2+} Loads. *Journal of Neuroscience Research*, **2001**. 66: p. 1019-1027.

89. Fuller, K.M. and E.A. Arriaga, Advances in the Analysis of Single Mitochondria. *Current Opinion in Biotechnology*, **2003**(14): p. 35-41.

90. Lu, H., et al., Micro Isoelectric Free Flow Separation of Subcellular Materials. *Micro Total Analysis Systems*, **2003**. 2: p. 915-918.

91. Legrand, O., et al., JC-1: A very Sensitive Fluorescent Probe to Test Pgp Activity in Adult Acute Myeloid Leukemia. *Blood*, **2001**. 97 (2): p. 502-508

92. Durrieu, F., et al., Synthesys of Bcl-2 in Response to Anthracycline Treatment May Contribute to an Apoptosis-Resistant Phenotype in Leukemic Cell Lines. *Cytometry*, **1999**. 36: p. 140-149.

93. Legrand, O., et al., JC-1: A very Sensitive Fluorescent Probe to Test Pgp Activity in Adult Acute Myeloid Leukemia. *Blood*, **2001**. 97 (2): p. 502-508.

94. Rabinovich, H., et al., Apoptosis-resistant Mitochondria in T cells Selected for Resistance to FAS Signaling. *The Journal of Biological Chemistry*, **2001**. 276(5): p. 3610-3619.

95. Rabinovich, H., et al., A Role for Mitochondrial Bak in Apoptotic Response to Anticancer Drugs. *The Journal of Biological Chemistry*, **2001**. 276 (36): p. 34307-34317

96. Mancini, M., et al., Mitochondrial Proliferation and Paradoxical Membrane Depolarization during Terminal Differentiation and Apoptosis in a Human Colon Carcinoma Cell Line. *The Journal of Cell Biology*, **1997**. 138 (2): p. 449-469.

97. Hirpara, J., M. Clements, and S. Pervaiz, Intracellular Acidification Triggered by Mitochondrial-derived Hydrogen Peroxide Is an Effector Mechanisam for Drug-Induced Apoptosis in Tumor Cells. *The Journal of Biological Chemistry*, **2001**. 276: p. 514-521.

98. Laurent-Crawford, A., B. Krust, and S. Muller, The Cytopathic Effect of HIV is Associated with Apoptosis. *Virology*, **1991**. 185: p. 829-839.

99. Laurent-Crawford, A., B. Krust, and Y. Riviere, Membrane expression of HIV envelope glycoprotein triggers apoptosis in CD4 cells. *AIDS Res Hum Retroviruses*, **1993**. 9: p. 761-773.

100. Pantaleo, G. and A. Fauci, Apoptosis in HIV Infection. *Nature Med*, **1995**. 1: p. 118-120.

101. Cossariza, A., et al., Mitochondria Alterations and Dramatic Tendency to Undergo Apoptosis in Peripherial Bloof Lymphocytes during Acute HIV Syndrome. *AIDS*, **1997**. 11: p. 19-26.

102. Srivastava, I.K., H. Rottenberg, and A.B. Vaidya, Atovaquone, a Broad Spectrum Antiparasitic Drug, Collapses Mitochondrial Membrane Potential in a Malarial Parasite. *The Journal of Biological Chemistry*, **1997**. 272(February 14): p. 3961-3966.

Chapter 2: Preliminary Experimental

2.1 Introduction

In this chapter, we present a series of studies, which led us to the final design and fabrication of the appropriate equipment for studying properties of subcellular components on chip. The equipment we developed included a multi-wavelength detection system and the appropriate software for data analysis. We also developed an in-house procedure for mitochondria isolation, using a variety of general protocols and adapting a protocol from the Rabinowich lab. Finally, we performed microfluidic experiments with cells and mitochondria and so developed the required expertise. Our initial experiments focused on cell viability assays on chip. They could be described as experiments in the "flow cytometry on chip" format. The application of this kind of experiment seemed very attractive for monitoring cell properties at the subcellular level. We then pursued the idea of monitoring mitochondria membrane potential ($\Delta\Psi_M$) using a similar experimental set-up. In the following sections, we explain the development of the appropriate equipment, which enabled our studies involving $\Delta\Psi_M$ change. A very important part of this chapter involves mitochondria isolation, which was done with the considerable assistance of Dr. Sandra Marcus.

2.2 Background Information on Reagents

2.2.1 Biological Samples

2.2.1.1 Introduction

All experiments have been performed with either Jurkat cells (ATTC No. TIB-152, clone E6-1, T cell leukemia, human) or mitochondria isolated from the same cell line. All the details related to cell culture and the protocol used for mitochondria isolation are described in the experimental section. In this section, we focus on general information about the protocols used for isolation of mitochondria.

2.2.1.2 Mitochondria isolation

There are different protocols enabling mitochondria isolation. The choice depends on the cell type, which is determined according to the function that cells have in an organism. Protocols are also designed according to the mitochondria activity that is studied in the specific experiment. Mitochondria are most often isolated from different mammalian tissues such as liver, heart, brain or skeletal muscle, rather than from cultured cells or yeast. Important information that can help to choose the cell type for mitochondria isolation is the mitochondria abundance. It is well known that fractions obtained from mammalian tissues and yeast are much more abundant in mitochondria, compared to the fractions obtained from cultured cells [1].

Each method of mitochondria isolation starts with cell lysis, which can be done using mechanical, gas, liquid shear or osmotic lysis. Most often this is done using liquid shear, where the suspension of cells is forced through a narrow space between the rotating pestle and the wall of the tube containing the cell suspension [2]. After homogenization, mitochondria purification will depend further on the mitochondria

activity, or on the physical properties that will be evaluated in the study. The mitochondria fraction must be free of any contaminants that could possibly interfere with their function or properties.

The simplest procedure for obtaining crude mitochondria fraction is differential centrifugation. After cell lysis is completed, low speed centrifugation is performed to remove non-lysed cells, nuclei and large membrane fragments. A higher speed centrifugation will pellet mitochondria. The resulting crude mitochondria pellet still contains some lysosomes, peroxisomes and membrane fragments. The crude pellet sometimes can be good enough for performing further studies [3].

If the crude preparation does not meet the desired purification level, it should be further purified by isopycnic centrifugation. The principle of this procedure is based on a separation due to density differences in the particles that are separated. During the separation on a density gradient, the particles will sediment or float up through the gradient until they reach the point in the gradient with the same density they have. Density gradients can be prepared from different media such as, for example, percoll, sucrose, metrizamide or nycodenz [2].

2.2.1.2.1 Evaluation of Fractionation

Once the procedure of mitochondria isolation is completed, it is necessary to quantify the amount of mitochondria in the fraction. In order to do that, it is necessary to determine the protein concentration and the activity of succinate dehydrogenase, which is a mitochondria enzyme marker.

2.2.1.2.2 Bradford Method

The Bradford method [4] is a commonly used assay for protein quantification in mitochondria isolation procedures. This method is based on the binding of Coomasie Brilliant Blue G-250 (CBB G-250; Figure 2-1) dye to a protein, causing a shift in the absorption maximum from 465 nm to 595 nm. The dye binds to bases (arginine most strongly) and aromatic moieties at a rate of approximately 1 mg of CBB per 1 mg of protein. After reading the absorbance, A_{595}, the sample protein concentration is determined by using a standard curve, which has been previously determined using standard solutions of BSA or IgG.

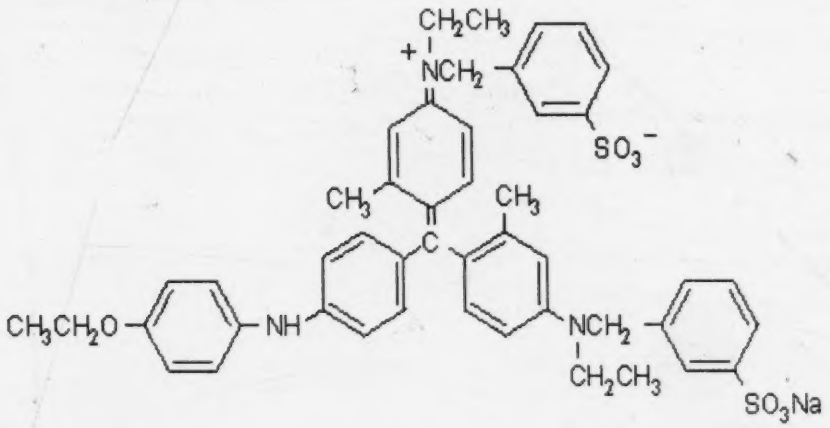

Figure 2-1. Structural formula of CBB G-250

cation	neutral	anion
470nm	650nm	595nm
red	green	blue

Table 2-1. Emission wavelengths of three forms of CBB G-250

2.2.1.2.3 Succinate – INT Reductase Assay

Succinate dehydrogenase is coupled with the coenzyme flavin adenine dinucleotide (E-FAD) and located in the inner mitochondria membrane. This complex is an iron-sulfur protein containing three different kinds of iron-sulfur clusters. It has an important role in the citric acid cycle, catalyzing the oxidation of succinate to fumarate (Figure 2-2), while reducing E-FAD to E-$FADH_2$. The electrons in $FADH_2$ stay within the complex being transferred to Fe-S centers of the protein and then to ubiquinone, for entry into the electron transport chain. The electron transport chain generates the proton motive force that drives the production of ATP (oxidative phosphorylation).

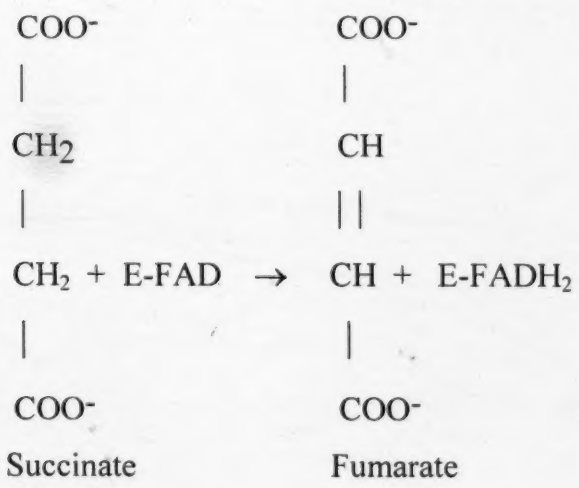

Figure 2-2. Oxidation of succinate to fumarate

In this assay, succinate reductase reduces iodonitrotetrazolium chloride (INT, Figure 2-3) to the colored product formazan, whose absorbance at 490 nm is measured by a spectrophotometer. The INT reductase assay is used to evaluate the activity of succinate INT reductase, which is indicative of the amount of mitochondria present in the preparation. A qualitative comparison of fractions can be made by comparing the ratio of absorbance at 490 nm to the amount of protein determined by the Bradford test. A more quantitative comparison can be done as explained by Munujos et al. [5]. Briefly, the activity of enzyme per mL of sample can be determined from the absorbance coefficient for formazan, and from the measured rate of absorbance change. The INT concentration should be high enough that there is no influence on the reaction rate (2mM in Munujos studies [5]).

It is important to mention that this test is best interpreted when it is certain that mitochondria are not damaged or their contents released in the isolation process. If succinate dehydrogenase is spread everywhere in the solution, the test will still give the succinate reductase activity, but the mitochondria will not be active.

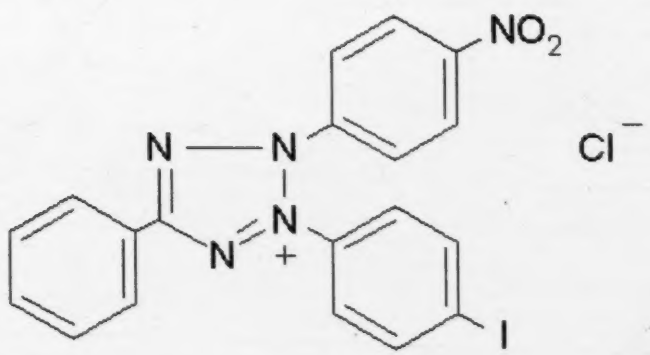

Figure 2-3. INT = 2-(4-Iodophenyl)-3-(4-nitrophenyl)-5-phenyl-2H-tetrazolium chloride (Adapted from Sigma-Aldrich Catalogue)

2.2.2 Sytox Green and JC-1 Stain

Sytox Green stain was purchased from Molecular Probes (catalogue number: S-7020). This nucleic acid stain easily passes through a damaged cell membrane, while it can not enter a cell with a healthy membrane. Excitation and emission wavelengths are 504 nm and 523 nm respectively.

JC-1 stain is also supplied by Molecular Probes (catalogue number: T-3168). Chemically it is 5,5',6,6'-tetrachloro1,1',3,3'tetraethylbenzimidazolyl- carbocyanine iodide.

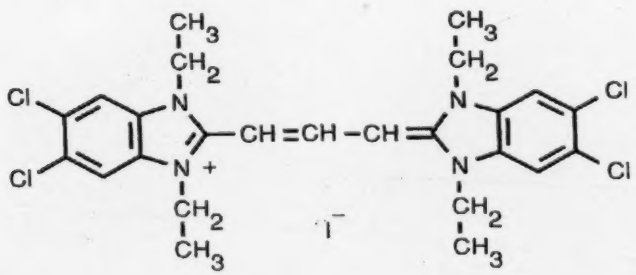

Figure 2-4. JC-1 = 5,5',6,6'-tetrachloro1,1',3,3'tetraethylbenzimidazolyl- carbocyanine iodide (diagram adapted from Molecular Probes catalogue)

The JC-1 molecule is a lipophylic cation (membrane-permeable). While monomers fluoresce in green (530 nm), aggregates give red fluorescence (595 nm). Once JC-1 stains mitochondria, it gives both red and green fluorescence simultaneously. When mitochondria are healthy, the negative membrane potential induces JC-1 aggregation, giving red fluorescence at high intensity. Damaged mitochondria give lower red fluorescence and either higher or the same green fluorescence, compared to healthy

mitochondria. Using the ratio of red/green fluorescence, it is possible to monitor depolarization of the mitochondria membrane when a cell is exposed to a drug.

2.2.3 Drugs Used for Treatment of Cells and Isolated Mitochondria

2.2.3.1 Valinomycin

Valinomycin is a cyclic amide ester. This neutral molecule consists of D-Valine, L-Lactate, L-Valine and D-Hydroxyvaleric acid (shown as A, B, C and D in Figure 2-5), with the sequence repeated three times. Valinomycin binds and shuttles K^+ ion across membranes. By transferring K^+ through the mitochondria membrane, the mitochondria membrane potential ($\Delta\psi$) is damaged, yet the ΔpH across the membrane is unchanged.

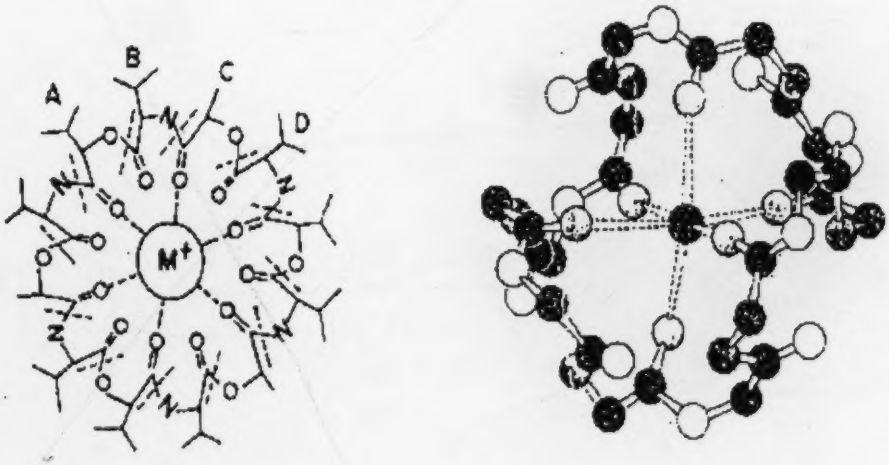

Figure 2-5. Structure of Valinomycin molecule. Adapted from Oxidative Phosphorylation Home Page (Univeristy of Leeds, UK)

2.2.3.2 Oligomycin

Oligomycin is a macrolide antibiotic that inhibits membrane-bound mitochondrial ATPase (F_0), preventing phosphoryl group transfer. It induces programmed cell death (apoptosis) causing chromatin condensation, changes in plasma membrane phospholipids, and a change in mitochondria membrane potential. The oligomycin used in these experiments was a mixture of oligomycin A (60%), B (30%) and C (10%), (Figure 2-6).

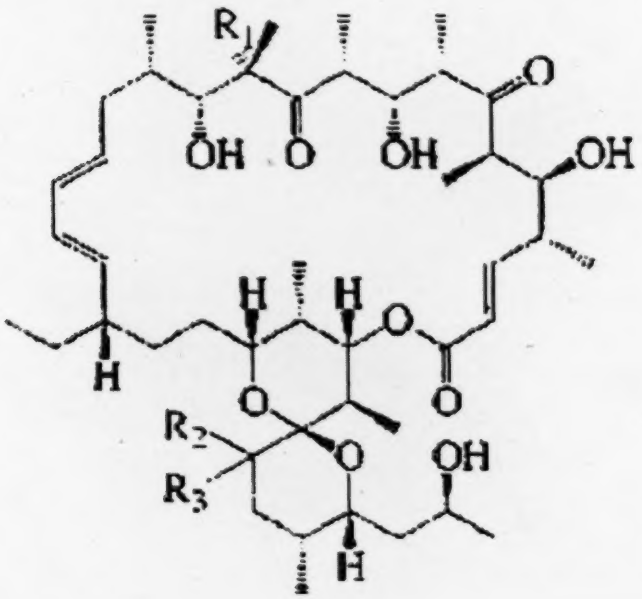

Oligomycin A, B, C

A: R_1 = OH; R_2 = R_3 = H

B: R_1 = OH; R_2, R_3 = O

C: R_1= H; R_2 = R_3 = H

Figure 2-6. Structure of Oligomycin molecule [6]

2.3 Experimental

2.3.1 Microfluidic device

2.3.1.1 Description of the Microfluidic Device

POCRE devices were used in all the experiments. This design was previously described and used by Wang and coworkers [7]. The layout of the device is shown in Figure 2-7. The chip was operated in the following way. Using a 100 μL pipette, a biological sample was transferred to the reservoir of the middle well, and the side well reservoirs were filled with 100 μL phosphate buffered saline (PBS). The fluid was introduced into channels by suction provided by a syringe pump (Harvard Apparatus, PHD 2000, Holliston, MA, USA) with a 100 μL SGE gas-tight syringe (Supelco, Bellefonte, PA, USA). The syringe was attached to the end of the waste channel using PTFE tubing of 13.4 cm length in a manner described earlier by Ocvirk and coworkers [8]. Channel F (shown in Figure 2-7) was not used. Cell viability experiments were done with devices of 70 μm channel depth and 150 μm channel top width. In monitoring $\Delta\psi_M$, devices with a channel depth of 30 μm and channel top width of 70 μm were used for cell experiments and devices of 70 μm channel depth were used for isolated mitochondria experiments.

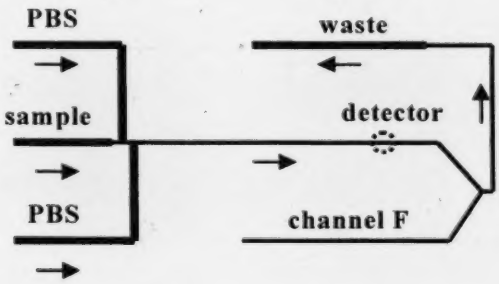

Figure 2-7. Layout of the PCRD1 device

2.3.1.2 Fabrication of Microfluidic Device

Microchips were fabricated from 4'' x 4'' 0221 glass (540 μm thick), (Corning, NY, USA) at the University of Alberta Nanofab. Fabrication was done using standard photolithographic and wet chemical etching techniques [9]. The procedure in the reference differs from the procedure we used in the following way. After the HPR 504 positive photoresist was deposited on the metal layers, the substrate was baked for 30 min. at 115 °C. The parameters used for thermal bonding are presented in the Table 2-2.

Program 3				
Mask	and	O221	glass	bonding
Stage	**1**	**2**	**3**	**4**
Rate (C degree/min)	10	2	2	4
Temp. (C degree)	440	473	592	473
Time (hours)	0.5	0.5	6	0.5

Table 2-2. The temperature program for thermal bonding

Once the chip was successfully bonded, reservoirs with a capacity of 100 μL, made from pipette tips, were glued on top of the outlet holes using RTV 108 silicone rubber adhesive sealant (General Electric Company, NY, USA).

2.3.2 Experimental Set Up

2.3.2.1 Components of the Experimental Set Up

A laser beam emitted by an air-cooled argon laser (488 nm, Cyonics, Uniphase 2014, San Jose, CA, USA) was directed by a set of mirrors (Newport, Irvine, CA, USA) through cylindrical lenses (focal lengths f_1 = 6.67 nm, f_2 = 80 mm; Melles Griot), which were used to broaden the beam into a band across the microchannel. The beam then entered a home-built epiluminescent microscope [8]; equipped with a dichroic mirror, focusing lens (25.4 mm diameter and 5.3 mm thickness) and mirror, from which the beam was directed into the channel of a microfluidic device. In order to detect fluorescence emitted by a stained cell or mitochondria in the channel, a microchip was clamped in a thick plexiglas holder above the microscope (Figure 2-9). The holder was connected to three XYZ translation stages (Newport 423, Irvine, CA, USA), which allowed XYZ translation of the device. The sample was moved through the microchannels using negative pressure provided by a syringe pump (Harvard Apparatus, PHD 2000, Holliston, MA, USA) with a 100 μL SGE gas-tight syringe (Supelco, Bellefonte, PA, USA). The syringe was connected to the outlet of the waste channels using PTFE tubing, as described in the reference [8]. We used single and multi-wavelength detection systems. Each system is described in detail below.

2.3.2.2 Single Wavelength Detection System

A single wavelength detection system was used in the cell viability experiments and in the initial studies of monitoring mitochondria membrane potentials. The system, initially developed for capillary electrophoresis peak detection, consisted of the home-built power supply, which was connected to the photomultiplier (Hammamatsu R1477 using a HC123-05 socket with an internal high voltage power supply and an internal high gain amplifier with 10^8 V/Amp gain and a 1 kHz low pass filter). Two photomultipliers (PMTs) of this kind were interchangeably used in the experiments. One was equipped

with 530DF30 filter (Omega Optical, part # XF3017) for detection of green fluorescence, while the one used for detection of red fluorescence was equipped with 605DF50 filter (Omega Optical, part # XF3019). The signal was further amplified with a 1700x gain amplifier, filtered (home built 4th order Bessel filter with a 25 Hz cutoff frequency) and captured with a National Instrument NB-MIO16-H data acquisition board, a MacIntosh computer and Lab View Software. Data were recorded using a sampling frequency of 500 Hz and averaging 10 data points, which gave a writing frequency of 50 Hz. Collected data were analyzed with Origin 7.0 on a PC.

Red and green photomultiplier tube housings were used interchangeably in the experiments for monitoring mitochondria membrane potential ($\Delta\psi$), as mitochondria fluoresced in both red and green. This system did not allow simultaneous recording of green and red fluorescence.

2.3.2.3 Multiwavelength Detection System

A multi-wavelength detection system enabled simultaneous recording of green and red fluorescence. A very important part of the system was a home-built optical connection for the PMTs (Figures 2-8 & 2-9). This part had built-in 505DRLP and 570DRLP dichroic mirrors (Omega Optical, part # XF2010 and #XF2015, respectively), which were used to separate red, green and laser (488 nm) wavelengths. A Photosensor Module (PMT) (Hammamatsu, Photonica, k.k., Type No. H6780-02) with a higher sensitivity for red fluorescence, and a built-in gain of 10^6 Volts/Amp, was used with the 605DF50 filter, while a PMT with a higher sensitivity for green fluorescence (Hammamatsu, Photonica, k.k., Type No. H5783, with a built-in 10^6 Volts/Amp gain) was used with the 530DF30 filter. The location of the filters and mirrors is shown in Figure 2-8. PMTs were connected to a home-built 0-10 V power supply with additional home-built amplifiers (3 outputs: 293,333 times, 29,333 times and 29,333 times gain) and electronic filters with a 5th order low-pass Bessel filter with a frequency of 100 Hz. This was designed and built by Kim Nguy at the Chemistry Electronic Shop of University of

Alberta. The signal was recorded using a PC computer (Celeron, 500 MHz) with National Instruments PC 1200 card (Celeron, 500 MHz) and a Labview program, using a sampling frequency of 10,000 Hz and averaging 4 data points to give a writing frequency of 2,500 Hz. Collected data were analyzed in Origin 7.0. Randy Tsen designed the Labview program used to record data from the multi-wavelegth detection system. He also modified Origin 7.0 in order to analyze these data.

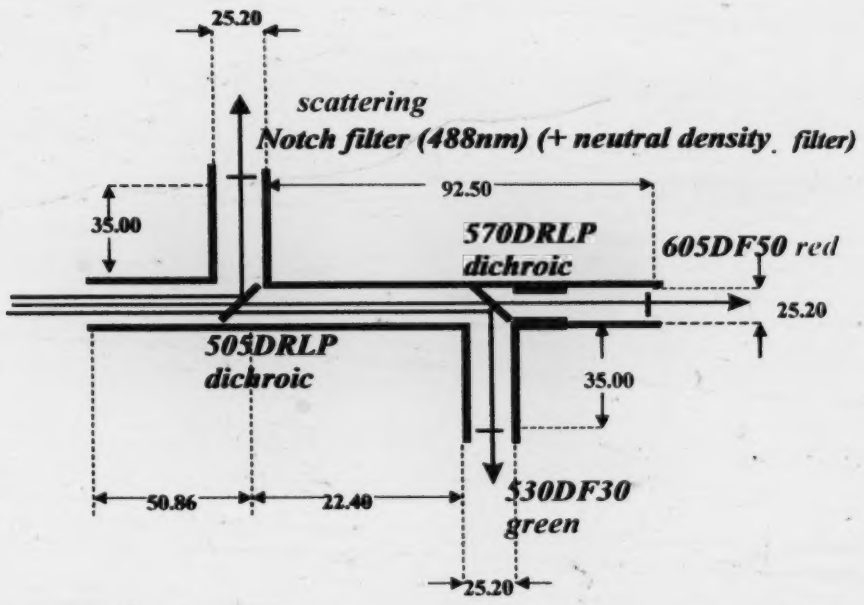

Figure 2-8. Schematic layout of the beam splitter that connects PMTs with the confocal microscope in the multi-wavelength detection system. Dimensions from the layout are expressed in mm. The inner diameter of the tubing that fits onto the microscope body was 25.20 mm, and a stop 19.00 mm in diameter was located 32.00 mm inside the tubing (not shown). Other details are shown in the appendix of the thesis.

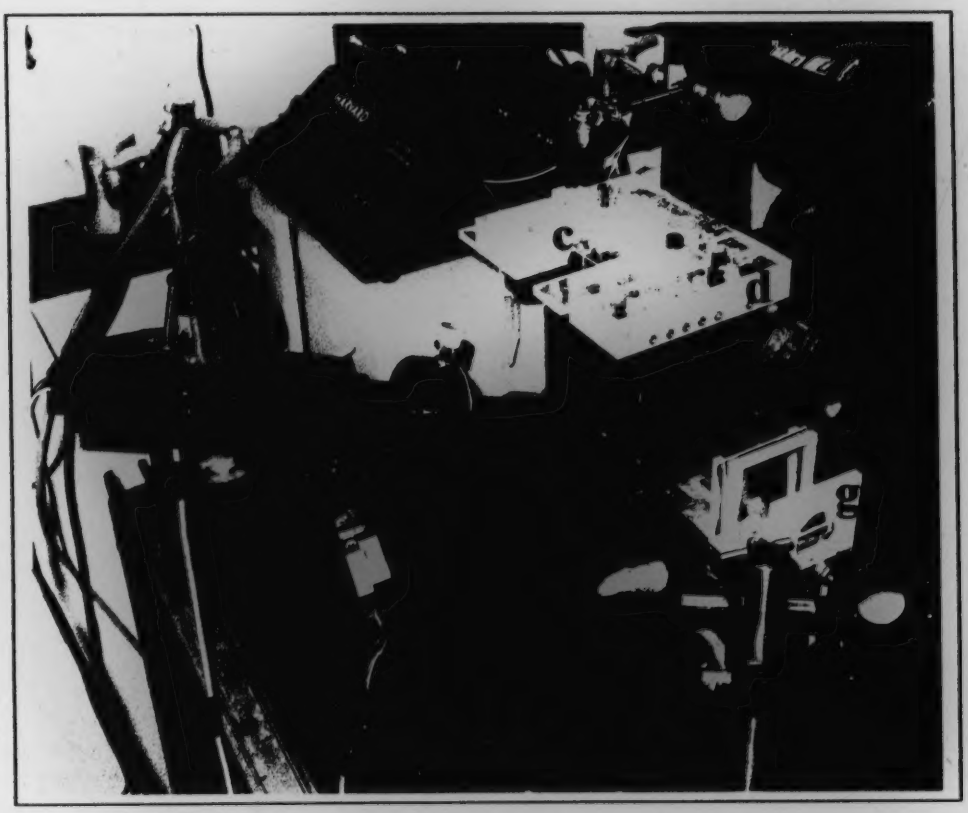

Figure 2-9. Experimental set-up. a) Connection part with 3 PMTs, b) Epiluminescent microscope, c) Microchip, d) Chip holder, e) Syringe pump, f) Ar laser, and g) Cylindrical lenses

2.3.3 Reagents and Chemicals

Phosphate buffered saline, PBS, which contains no calcium or magnesium (cat.# 14190-144) was purchased from Gibco, Life Technologies, Inc. Media for culturing cells RPMI (Roswell Park Memorial Institute) 1640 (cat.# R-8758), Fetal Bovine Serum (cat # F-2442), antibiotic-antimycotic solution (10,000 units/mL penicillin, 10 mg/mL stroptomycin and 25 μg/mL amphotericin B 25) and L–glutamine were all obtained from Sigma-Aldrich. Trypan Blue 0.4 % solution (Sigma-Aldrich) was used to determine cell viability. UV purified water (mQ water) was produced by MiliQ UV Plus apparatus (Milipore, S.A. 67120, Molsheim, France) containing de-ionizing columns, carbon filter and UV-purification. Ethanol solution (70%), which was used for flushing the microchip channels was prepared with miliQ water and filtered (Milipore filters, Bedford, MA, USA) before introducing into the chip. Bleach solution (10%) prepared with distilled water was used overnight for the disposal of biological material remaining after the experiment. Sytox Green Stain and JC-1 stain (5, 5', 6, 6'-tetrachloro1, 1', 3, 3'tetraethyl-benzimidazolyl-carbocyanine iodide) were purchased from Molecular Probes (cat # S-7020 and cat. # T3168, respectively). Stock solutions of both stains were made with dimethyl sulfoxide (DMSO; Caledon Laboratories Ltd, George town, ON, Canada). JC-1 stock solution of 1 mg/mL was kept in the freezer at –20 °C, while Sytox Green stock solution of 100 μM was kept in the fridge at +4 °C in the fridge. Mitochondria and cells were treated with Valinomycin (Sigma- Aldrich) or Oligomycin (from Streptomyces diastatochromogenes; a mixture of Oligomycin A (60%), B (30%) and C (10 %); Sigma-Aldrich, cat.# 75352). Buffers used in the mitochondria isolation procedure were homogenization buffer, HB (10 mM triethanolamine-acetate (pH 7.4), 0.25 M Sucrose (isotonic), 1 mM EDTA and 4 mM KH_2PO_4) and mitochondria buffer, MIB (10 mM MOPS (pH 7.4, adjusted with HCl), 0.25 M Sucrose (isotonic), 1mM EDTA and 4 mM KH_2PO_4). Protease inhibitor cocktail tablets (Roche Diagnostics GmbH, cat. # 1873580) were added to the sample during isolation, while fatty acid free bovine serum albumine, FAF BSA (lyophilized powder, Sigma-Aldrich, cat. # A6003) was added to the isolated mitochondria before freezing for storage at – 70 °C. Isopycnic centrifugation was done on a Percoll (Sigma-Aldrich, cat. # P1644) gradient. The evaluation of the fractionation was

done by Bradford Assay (Biorad Protein Assay) and succinate dehydrogenase assay, where we used succinate (0.01 M in 0.05 Na-phosphate buffer) and INT-iodonitrotetrazolium chloride (Sigma-Aldrich, cat.# I8377; 2.5 mg/mL in 0.01M succinate in 0.05 Na-phosphate buffer).

2.3.4 Cell Culture

Jurkat cells (ATTC No. TIB-152, clone E6-1, T cell leukemia, human) were cultured in RPMI 1640 media supplemented with 2 % antibiotic antimycotic solution, 10 % fetal bovine serum and 1 % L-glutamine 200 mM. The cells were maintained at a concentration of approximately 1 x 10^6 cells/ml in a humidified atmosphere at 37 °C and 8% CO_2, provided by an incubator (NuAir US Autoflow (NU-4750) Automatic CO_2 water-jacketed incubator (Plymouth, MN, USA)). Their concentration was determined by hemacytometer (Sigma-Aldrich, Oakville, ON, Canada). A dye exclusion test using 0.4% Trypan Blue solution was used to determine cell viability. The average percentage of viable cells in the solution was in the range of 91-94 %.

2.3.5 Mitochondria Isolation

Mitochondria were isolated from Jurkat cells following a protocol designed according to references [1], [2], [10], [3], [11].

2.3.5.1 Isolation Protocol

1. Grow 500 ml Jurkat cells to 1x 10^6 cells per mL (5x10^8 total cells).
2. Pellet cells in the Beckman JA10 rotor at 1000 g_{max} (2500 rpm) for 10 min at room temperature. Decant the supernatant and disrupt the pellet.

3. Suspend cells in 80 mL serum-free RPMI medium. Transfer to two 50 mL conical tubes.

4. Centrifuge in the Rotofix 32 centrifuge with a Hettich 1624 rotor (swing-bucket rotor) at 3100 rpm (1500 g_{max}) for 10 min.

5. Aspirate the supernatant and disrupt the cell pellets by flicking the tube. Resuspend each in an additional 4 mL serum-free medium and transfer to a single 15 mL tube. Wash the tubes with 4 mL media and combine into the same tube. Mix and then divide into two tubes. Centrifuge in the benchtop centrufuge at 3100 rpm for 10 min. Aspirate the supernatant to remove the entire medium.

6. Suspend the cells in homogenization buffer (HB) in a volume equal to 6 times the packed cell volume and add 1x protease inhibitors (using 25 x stock). Transfer to the loose-fitting Dounce homogenizer (Wheaton type B Pestle, 15 mL size).

7. Let the cells sit on ice for 15 min. to weaken the cell membranes. Keep on ice from this point on, and do all centrifuging in a cold rotor.

8. Homogenize with 40 strokes. Check cells under microscope to see the extent of breakage, compared to the untreated sample (10 µL diluted in 40 µL PBS). There should be more than 80% free nuclei. If not, switch to the tight Dounce pestle (Wheaton type A Pestle, 15 mL) and homogenize in 10 stroke increments, checking in between, to a maximum of 40 strokes. Add 1/20 volume BSA in HB to give 0.5 mg/mL final.

9. Transfer to a 15 mL tube. Centrifuge in cold room at 3350 rpm (1750 g_{max}) for 5 min.

10. Transfer the supernatant to a fresh tube. Suspend the pellet in an additional 4 mL HB using 3 strokes of the loose-fit Dounce. Centrifuge both tubes as in step 9. Combine the two supernatants and transfer to a fresh tube. Centrifuge again as in step 9 to completely remove the nuclei.

11. Centrifuge at 20,000 g_{AV} (17 000 rpm) for 15 min at 4 °C in the Beckman centrifuge with a 70.1 type ultracentrifuge rotor to pellet mitochondria.

12. If the goal of the isolation is to obtain crude mitochondria prep, proceed with step 13 as a final step. If mitochondria are to be purified on Percoll gradient, skip step 13 and proceed to step 14.

13. First suspend crude mitochondria in 3 mL of MIB. To suspend, transfer the pellet to the 7 mL loose–fit Dounce and suspend with 2 gentle strokes of the pestle. Assay the protein concentration using the Bradford method and sometimes we performed the succinate activity assay. Pellet the mitochondria at 14,000 rpm (16,000 g) in a benchtop microcentrifuge. Suspend at 3-5 mg/mL in MIB + 10 mg/mL FAF BSA and split into aliquots. Snap freeze in a dry ethanol bath. Transfer to the -70 °C freezer for storage.

14. Resuspend pellet in 3 ml MIB using 2 gentle strokes in a loose-fit Dounce homogenizer. Keep on ice until Percoll gradient is ready.

15. Prepare the following Percoll dilutions using MIB without protease inhibitors:

    a) 4 mL 70% Percoll in MIB (2.8 mL of Percoll + 1.2 mL MIB)

    b) 4 mL 30% Percoll in MIB (1.2 mL of Percoll + 2.8 mL MIB)

    c) 4 mL 18% Percoll in MIB (0.72 mL of Percoll + 3.28 mL MIB)

    d) 4 mL 10% Percoll in MIB (0.4 mL of Percoll + 3.6 mL MIB)

16. Make Percoll layers in Type 70.1 Ti centrufuge tubes (thick-walled polycarbonate no. 355630). Start with the heaviest percoll. Using 3 cm^3 syringe, layer 1.5 mL each. Keep the tube slanted and trickle through the needle very slowly down the side of the tube to make the layers. Layer 1.5 mL of mitochondria suspension on the top. Make two tubes (each will have 7.5 mL). After each layer, mark the interface.

17. Centrifuge in the type 70.1 Ti rotor in the Beckman ultracentrifuge at 15 000 g_{max} (13 000 rpm) for 13 min.

18. Collect the mitochondria at the 30/70 interface with a Pasteur pipette or blunt needle. Before diluting, take a sample of the "mitochondria" band and sample at the 10/18 interface for comparison. During the next centrifuge, do a succinate –INT reductase assay.

19. Dilute mitochondria 10-fold in MIB + 1 mg/mL FAF BSA. Transfer to a JA20 tube and centrifuge in the JA20 rotor for 30 min at 22 000 g_{max} (13500 rpm).

20. Resuspend mitochondria in 1mL MIB (using Dounce with loose-fit pestle as in step 13) and transfer to a 1.5 mL tube. Take a sample for Bradford and succinate (INT) reductase assays to determine the protein concentration and succinate activity.

21. Centrifuge at 10 000 g_{av} for 10 min. in microfuge.

22. Resuspend the final pellet in 0.5 mL MIB + 10 mg/mL FAF BSA.

23. Divide in aliquots and then snap freeze them in a dry ice ethanol bath. Transfer to the -70 °C freezer for storage.

2.3.5.2 Bradford Assay and Succinate INT Assay

A Bio-Rad Protein Assay (Bradford method) was used to determine protein concentration in the sample of isolated mitochondria. Sample (10 µL) was mixed with 500 µL of Protein Assay Dye Ready-to-use Reagent (catalogue # 500-0006), incubated 5 min. at room temperature and then the absorbance was read at 595 nm. The absorbances of BSA solutions of known concentrations (0.05, 0.1, 0.2, 0.35 and 0.5 mg/mL) gave a standard curve (A_{595} vs. $conc._{protein}$, mg/mL), from which the protein concentration of the mitochondria sample was easily evaluated.

NOTE: If a frozen sample is tested, it is necessary to remove 10 mg/mL FAF BSA before the Bradford assay. The sample should be centrifuged at 14,000 rpm for 5 min. in order to pellet mitochondria and then the pellet should be suspended in MIB.

A succinate (INT) reductase test was performed in the folllowing way. Isolated mitochondria sample (50 μL) was incubated in 0.5 mL of 0.01 M succinate and 0.2 mL of INT (2.5 mg/mL) at 37 °C for 10 min. After this, the absorbance was read at 490 nm. The results were compared qualitatively as described in section 2.2.1.2.3.

2.3.6 Cell Viability

Cell viability experiments were performed with Jurkat cells using Sytox Green stain and 70% ethanol. Cells at a concentration of 1 x 10^6 cells/mL were incubated with 70% alcohol for 60 min. Then they were pelleted at 2000 rpm for 10 min. in a Sanyo MSE MicroCentaur centrifuge and resuspended in RPMI 1640 media supplemented with 2 % antibiotic antimycotic solution, 10 % fetal bovine serum and 1 % L-glutamine 200 mM. Cells treated with alcohol were then incubated with 1 μM Sytox Green stain for 20 min, washed twice with PBS, suspended in PBS and introduced into the middle well of the microchip device (70 μm deep channels) for fluorescence detection. The sample was drawn through the microchannel using negative pressure provided by the syringe pump (Harvard Apparatus, PHD 2000, Holliston, MA, USA) with a 100 μL SGE gas-tight syringe (Supelco, Bellefonte, PA, USA). Each run lasted 60 seconds and the flow rate used in the experiment was 0.1 μL/min. Green fluorescence signal was detected with the single-wavelength detection system, which was described in detail in section 2.1.4.2. Data were collected using a LabView program with a sampling frequency of 500 Hz, averaging of 10 data points and writing frequency of 50 Hz. Recorded data were analyzed in Origin 5.0. After an experiment was completed, the microchip device was thoroughly flushed with 70% ethanol and mQ water (produced by Mili Q, Milipore S.A. 67120, Molsheim, France). The biological material that remained was disposed of in 10 % bleach.

2.3.7 Test Experiments for Monitoring $\Delta\psi_M$

Test experiments for monitoring mitochondria membrane potential ($\Delta\psi_M$) were performed with Jurkat cells at concentrations of 1 x 10^6 cells/mL, treated either with 70 % ethanol or 10 μM valinomycin for 30 min. Cells were then spun at 2,000 rpm in a Sanyo MSE MicroCentaur centrifuge for 10 min. and suspended in RPMI 1640 media. They were incubated with 10 μg/mL JC-1 stain, washed twice, and then resuspended in PBS buffer. After that, 100 μL of sample was pipetted into the reservoir of the middle well in the POCRE chip (device with 30 μm deep channels), while the two side reservoirs were filled with 100 μL of PBS buffer. The fluid was drawn through the microchannels by negative pressure flow provided by the syringe pump (Harvard Apparatus, PHD 2000, Holliston, MA, USA) with a 100 μL SGE gas-tight syringe (Supelco, Bellefonte, PA, USA). Each run lasted 60 seconds and the flow rate used in the experiment was varied for different runs: 0.1, 1, 3, 5, 10 and 100 μL/min. The single-wavelength detection system was used to record the fluorescence signal. Red or green signals were recorded one after another in runs of 60 seconds. Data were collected using a LabView program with sampling frequency of 500 Hz and a writing frequency of 50 Hz. Recorded data were analyzed in Origin 5.0. After an experiment was completed, the microchip device was thoroughly flushed with 70% ethanol and mQ water (produced by Mili Q, Milipore S.A. 67120, Molsheim, France) by applying vacuum at the waste outlet.

2.3.8 Data Capture and Analysis

2.3.8.1 Oscilloscope Data Capture – Hardware Testing

The biological samples used in these experiments were healthy Jurkat cells (1 x 10^6 cells/mL) and mitochondria (protein concentrations: crude = 1.17 mg/mL, Percoll purified, Fraction A = 0.3 mg/ mL and Fraction C = 0.2 mg/mL) isolated from the same cell line. Aliquots of the biological sample (100μL) were thawed and diluted to 1 mL with MIB (10 mM MOPS (pH 7.4, adjusted with HCl), 0.25 M Sucrose (isotonic), 1 mM EDTA, 4 mM KH_2PO_4). Cells were stained by incubation with 10 μg/mL JC-1 for 10 min., washed twice and then resuspended in phosphate buffered saline (PBS), while mitochondria were incubated with 10 μg/mL JC-1 stain for 2 min., washed twice and then resuspended in PBS. The sample was introduced into a microchip by negative pressure flow using a syringe pump (Harvard Apparatus, PHD 2000, Holliston, MA, USA) with a 100 μL SGE gas-tight syringe (Supelco, Bellefonte, PA, USA).

An oscilloscope (Tektronix 2430, Portland, Oregon, USA) was used to determine the preferred cut-off frequency for a low pass frequency filter. In this experiment, Jurkat cells stained with JC-1 flowed through 30 μm deep channels at 5 μL/min. Using a Krohn-Hite 4-pole filter to set various frequencies, raw signal was compared with signals filtered at 25 Hz, 50 Hz, 80 Hz and 100 Hz.

An oscilloscope was also used to test PMT units (Hammamatsu, Photonica, k.k., red sensitive - PMT, Type No. H6780-02 and green sensitive - PMT, Type No. H5783). For these experiments, we used both cells and isolated mitochondria flowing through the microchip at a rate of 1 μL/min.

2.3.8.2 Software Testing

Software designed for monitoring MMP was tested using cells flowing at a rate of 5 μL/min. These experiments helped us to pick an optimized frequency for collecting data and for the averaging rate of the data collection.

2.4 Results and Discussion

2.4.1 Mitochondria Isolation

Mitochondria were isolated according to the protocol described in the Section 2.3.5. Half of the material was saved as a crude prep and the rest was purified on percoll gradient. After separation on the gradient, there was no band at the 30/70 interface as was expected [10]. Instead, the band was lifted and separated into two bands (B, C). There was another thin band (A) above these two (Fig.2-10). All three bands were removed by a Pasteur pipette and samples were taken for Bradford assay and succinate dehydrogenase assay (Table 2- 3).

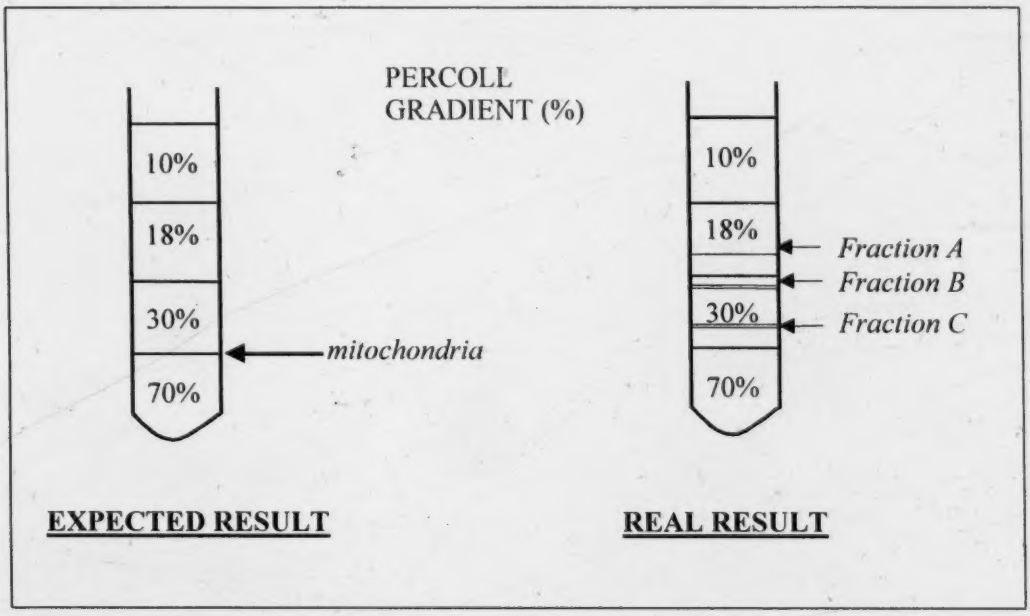

Figure 2-10. Mitochondria Isolation on Percoll Gradient

Isolation No.		Protein (mg/mL)	INT reductase A490	Volume of aliquots for storage (μL)
1	crude 1	1.78	0.21	100
	crude 1a	1.85	0.3	100
2	crude 2	1.17	0.31	100
	fraction A	0.28	0.063	100
	fraction B	0.49	0.246	100
	fraction C	0.21	0.095	100
3	crude 3	3.8	/	50

Table 2-3 Table shows the results from the Bradford and succinate dehydrogenase assay for all the mitochondria samples we used in the experiments

Using these results, we compared the fractions and came to the conclusion that fraction B (isolation 2) gave the greatest abundance of enriched mitochondria when they were isolated on a Percoll gradient (Table 2-3). After examining the red/green signal ratio of the different fractions using the JC-1 stain, we decided to perform most of the experiments with crude mitochondria. The crude preparation showed selective JC-1 staining of mitochondria. The Percoll gradient separations were time consuming, and the volume of the sample containing isolated mitochondria was very small. Fraction B from isolation 2 was used for an experiment in which the $\Delta\psi_M$ drop was compared for cells and isolated mitochondria treated with valinomycin. Fractions A and C were used in test experiments for the multi-wavelength detection system. All other experiments were performed with crude mitochondria, which had comparable succinate activity.

We note that the lower purity of the crude mitochondria isolate is indicated by a much higher protein concentration compared to mitochondria isolated on Percoll

gradient. It is possible that this high protein content accounts for the greater tendency of the crude mitochondria preparation to clog channels compared to mitochondria isolated on Percoll. However, this hypothesis was not tested.

2.4.2 Cell Viability

Jurkat cells (1 x 10^6 cells/mL) were treated with 70% ethanol for 60 min. and stained with 1 μM Sytox Green (dead cell stain). Cells were introduced into a microchip with 70 μm deep channels, using suction at 0.1 μL/min. Based on the cross sectional area, the average linear velocity was 0.02 cm/s. The peak width was theoretically expected to be 0.2 s and the experimentally obtained peak widths are in agreement (Figure 2-11). The estimate is based on a laser line of ~ 10 μm, and a cell diameter of 15 μm, giving total detector cell transit length of 30 μm. Figure 2-11 shows the trace of 76 dead cells detected using green fluorescence detection during a 60 s run. These results demonstrated the ability to detect and count dead cells in a flowing stream within a microchip using Sytox Green. Using a color video camera, we also captured images of cells flowing through microchannels and recorded them by VCR (Figure 2-12a, and Figure 2-12b).

The results of these cell viability pilot experiments showed that cell viability assays on chip are possible. In the period that we were developing the technique, Ramsey and coworkers published a similar flow cytometry on chip study [12], using E.Coli stained with propidium iodide and Syto 15 dyes. Our cell viability experiments are in agreement with their results in terms of establishing the use of chips for cell viability determination by flow cytometry.

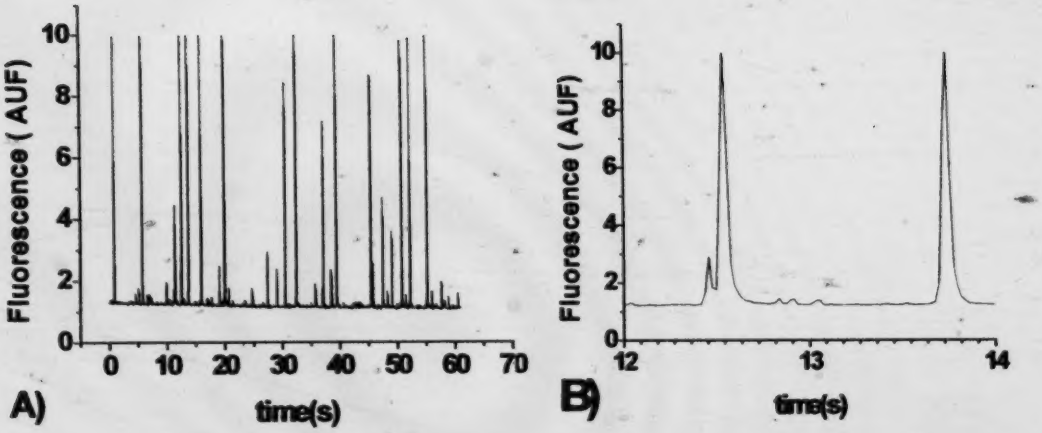

Figure 2-11. Trace of dead Jurkat cells stained with 1 μM Sytox Green. Experimental conditions: flow rate of 0.1 μL/min, 70 μm deep chip channels, 1 x 10^6 cells/mL. Fluorescence shown in the trace is expressed in arbitrary units of fluorescence (AUF). A) 60 s run; B) expansion of 2 s run; peak width is close to 0.2 s

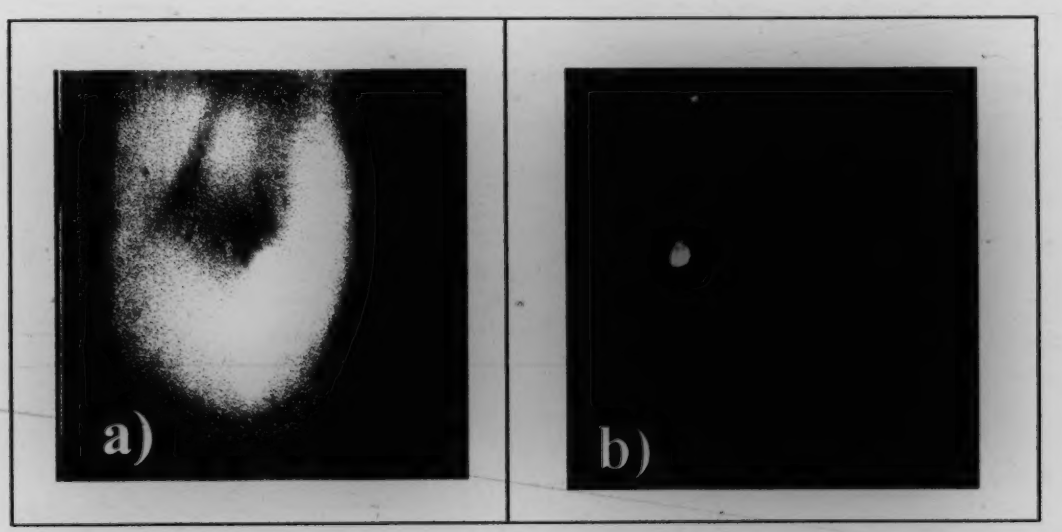

Figure 2- 12. Both image a) and b) show dead Jurkat cells flowing through the 70 μm deep microchannels. a) Vertical green lines are channel walls; the distance between them is 150 μm; the picture is taken with added white light, so the channel walls could be seen. b) The same image as in a) but no white light added.

2.4.3 Test Experiments for Monitoring Mitochondria Membrane Potential

Test experiments for monitoring mitochondria membrane potential ($\Delta\psi_M$) were performed with Jurkat cells (1 x 10^6 cells/mL) treated either with 70 % ethanol or 10 μM valinomycin for 30 min., stained with JC-1 and introduced into a microchip with 30 μm deep channel (cross section 1713 x 10^{-8} cm^2) for fluorescence detection. The flow rate was 1 μL/min, so the average linear velocity was 1 cm/s. Detection was performed with the single-wavelength system, which did not enable simultaneous detection of red and green fluorescence. Satisfactory traces were obtained for both red and green fluorescence, as shown in Figures 2-13a & 2-14a. However, the calculated peak width of 0.004 s did not correspond to the experimentally obtained peak width of 0.1 s (Figures 2-13b & 2-14b). A detector cell transit length of 40 μm was used. Also, the ratio of red/green fluorescence intensity appeared to vary randomly between samples and the controls (untreated cells). All this could be attributed to the detection system that recorded data with a data writing frequency of only 50 Hz and the use of a 25 Hz low pass filter. These choices were originally made for acquisition of capillary electrophoresis data, but were totally inappropriate for the very rapid peaks seen with pressure driven pumping of mitochondria or cells. The inability to obtain simultaneous recording of both red and green fluorescence also made it difficult to compare intensities. As a result, a multi-wavelength system, with better data acquisition parameters was developed. Section 2.3.2.3. explains the improvements of the detection system, which enabled direct comparison of the data at two wavelengths.

In test experiments for monitoring $\Delta\Psi_M$, we also captured images of stained mitochondria from Jurkat cells fluorescing in red. Images were taken by a color video camera and recorded by VCR (Figure 2-15)

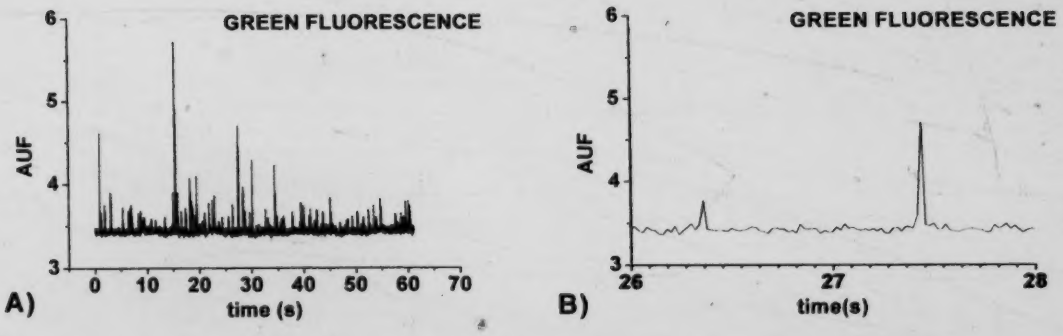

Figure 2-13. Green fluorescent signal from Jurkat cells treated with 70% ethanol and stained with JC-1. Flow rate was 1 μL/min. The signal was recorded with single-wavelength detection system. A) 60 s run, B) 2 s run extracted from 60 s run shown at left

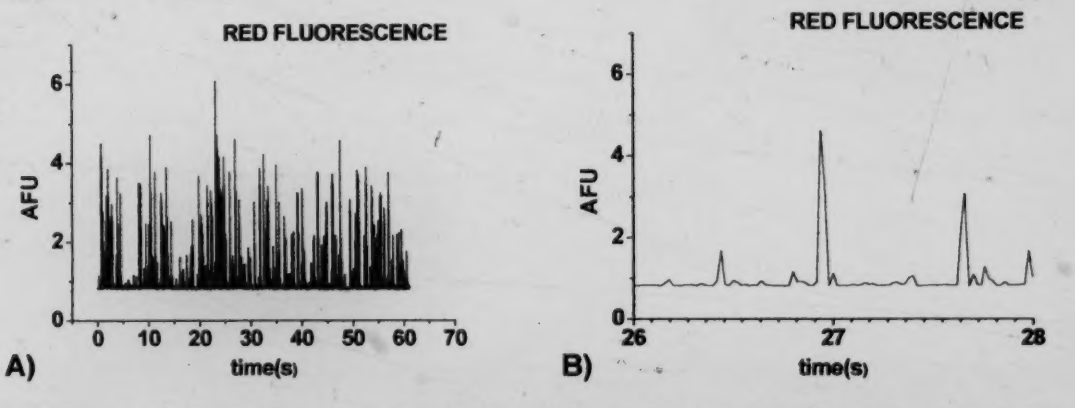

Figure 2-14. Red fluorescent signal from Jurkat cells treated with 70% ethanol and stained with JC-1. Flow rate was 1 μL/min. The signal was recorded with single-wavelength detection system. A) 60 s run, B) 2 s run extracted from 60 s run shown at left

Figure 2-15. The picture of stained healthy mitochondria within whole Jurkat cell was taken by a color video camera (TK-1280U, JVC, Japan) equipped with 590DRLP filter.

2.4.4 Data Capture and Analysis

2.4.4.1 Oscilloscope Data Capture – Hardware Testing

An oscilloscope was used to capture the raw PMT data and to compare it to the low pass filtered data. New equipment that was built specifically for the monitoring of $\Delta\psi_M$ in cells and isolated mitochondria stained by JC-1 was tested to ensure good quality peak measurements. New, small light photomultipliers were tested to determine the appropriate amplifier gain and PMT voltages. In the cell experiments we used chips with 30 μm deep channels and in mitochondria experiments 70 μm deep channels were used.

The raw PMT signal was compared to the results obtained with a Krohn-Hite 4-pole filter, set to frequencies of 25, 50, 80 and 100 Hz. At a flow rate of 5 μL/min, and a cell concentration of 1 x 10^6 cells/mL, a typical baseline peak width of 20-30 ms/cell was seen for the raw data of JC-1 stained cells. Occasionally, peak widths of 40 – 60 ms were also observed. The full width at half maximum (FWHM) was typically 10 - 14 ms. The peak heights were up to 2.7 V with 500 V on the R1477 PMT and 1,700 times gain. The noise was about 250 mV peak to peak (p to p). With the filter in place and set to 25 Hz low pass, maximally flat (i.e. a Bessel filter), the baseline peak widths were typically 75 ms wide, peak heights were 1- 1.5 V, and the p to p noise was about 20 mV. With an 80 Hz filter the peak widths were 30 – 45 ms and the p to p noise was 30 – 40 mV. With a 100 Hz filter the peaks were better resolved, with about 30 ms peak widths, and similar noise levels. We concluded that a 100 Hz filter gave a good compromise between peak distortion and lowered noise at a 5 μL/min flow rate. When the flow rate was increased to 100 μL/ min and peaks narrowed to 10 ms in the raw data, there was significant peak distortion seen with the 100 Hz filter. The R1477 PMT had a built-in filter with a 1 kHz bandwidth, giving a time constant of around 1 ms. The flow rate of 5 μL/min in a 30 μm deep chip channel should have given peak widths for cells of about 1 ms. The observed peaks were perhaps larger, partly due to the cell sampling different velocity profiles across the channels, and in part due to the time constant of the PMT.

The testing of the H6780-02 and H5783 PMTs was performed at a flow rate of 1 μL/min with both cells (1 x 10^6 cells/mL) and mitochondria (protein concentrations: crude = 0.12 mg/mL; Percoll purified, Fraction A = 0.03 mg/ mL; Fraction C = 0.02 mg/mL) stained with 10 μg/mL JC-1 stain. Oscilloscope traces for green signals filtered with 5th order 100 Hz low pass filter and amplified 22,000 times are shown in Figures 2-16 & 2-17 for cells and for crude mitochondria. Similar results were obtained for Percoll purified mitochondria fractions A and C but were not shown here. An estimate of the peak width for cells based on the average velocity in 30 μm deep microchannels is about 4 ms, given a detector transit length of 40 μm. The data in Figure 2-16 shows baseline widths of about 15 ms and FWHM values of 5 ms or less. These PMT modules did not have an internal filter. For the much smaller mitochondria a peak width of about 3-4 ms can be estimated, given a detector transit length of ~ 10μm. Thus, the 100 Hz filter should broaden these peaks. The much sharper baselines seen in Figure 2-17 compared to Figure 2-16 for cells is consistent with these expectations. The green fluorescence signal from isolated mitochondria was much lower in intensity compared with the red fluorescence intensity. These test experiments allowed us to select the PMT voltage and amplifier gains for the multi-wavelength detection that was used in all later experiments (Table 2- 4).

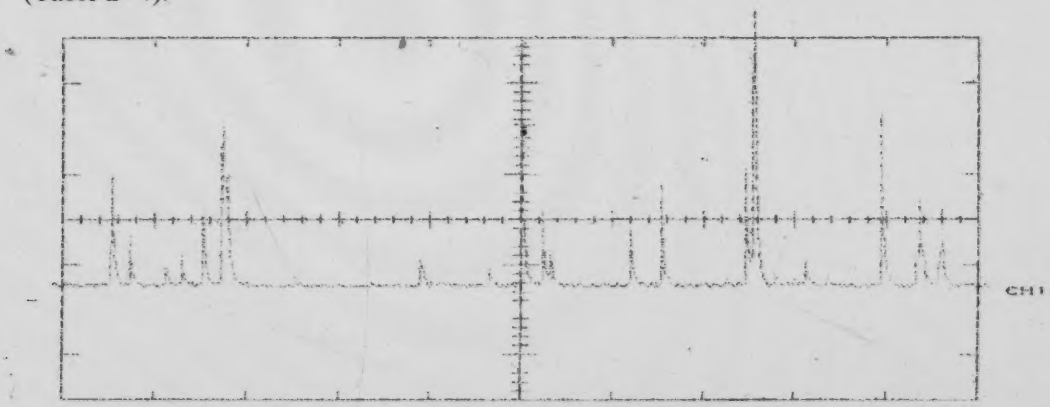

Figure 2-16. Oscilloscope trace shows green fluorescent signal from healthy Jurkat cells (1 x 10^6 cells/mL) stained with 10 μg/mL JC-1. X-axis divison is 100 ms and Y-axis division is 1V. Flow rate used was 5μL/min and the PMT was set at 500 V with a 15 x gain.

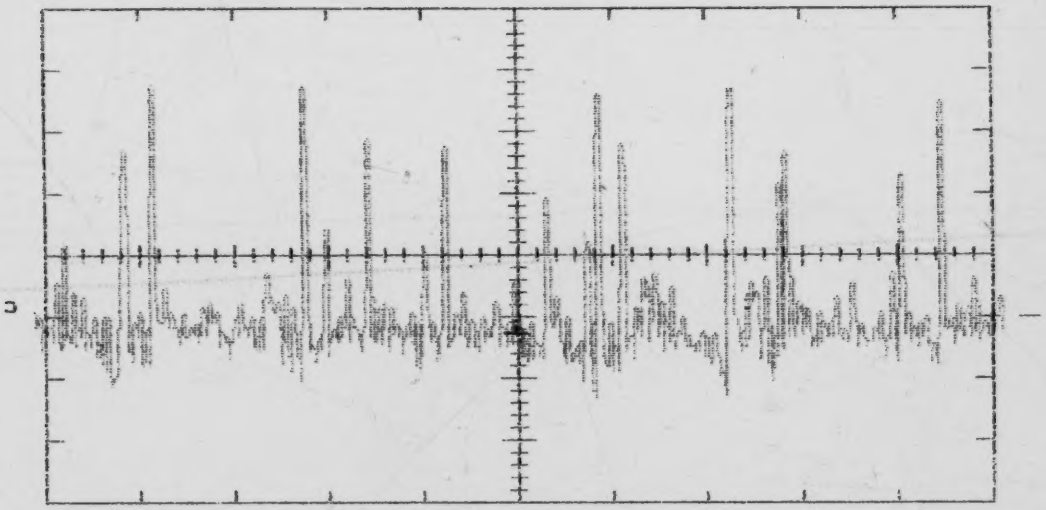

Figure 2-17. Oscilloscope trace shows green fluorescent signal from healthy crude mitochondria (protein concentration 0.12 mg/ mL) stained with JC-1 (10 μg/mL). X-axis division is 100 ms and Y-axis division is 10 mV. Flow rate used was 1 μL/min and PMT was set at 500 V with a 15 x gain.

	PMT (Volts)		Amplifier gain	
	red	green	red	green
cells	550	550	20x	20x
mitochondria	750	750	20x	200x

Table 2-4. PMT voltages and amplifier gains found to be the most appropriate for the experiments of $\Delta\psi_M$ monitoring in cells and isolated mitochondria

2.4.4.2 Software Testing

A LabView program was developed for collecting data with the multi-wavelength detection system, which enabled simultaneous recording of the red and green fluorescence emitted from the cells or isolated mitochondria stained with JC-1 stain. In order to determine the proper frequency for collecting data, we tested the system using Jurkat cells (1×10^6 cells/mL) stained with 10 μg/mL of JC-1 flowing through 30 μm deep microchannels at 5 μL/min. In the first set of the experiments, the frequency of collecting data used for the following values was 1, 2, 3, 4, 5, 10, 15 and 20 kHz, and two data points were averaged, for a writing rate of half those values. At 10 kHz and above the signals were properly captured. At 4 kHz or below, peaks were occasionally missed or were distorted. In order to minimize the size of data files and improve the signal to noise ratio, we also tested the best averaging rate. Averaging of 2, 4, 6 and 8 data was tested at different sampling frequencies. These tests resulted in a final frequency selection for collecting data at 10,000 Hz then averaging 4 data points, giving a writing frequency of 2,500 Hz. This combination offered good quality data, compromising between the size of the data file and proper description of the data recorded (high averaging rate can lead to distortion of the data recorded).

Recorded data were analyzed in Origin 7.0, which was modified to determine the maximum of the red peaks and their coincident green peaks. Both red and green peak heights (quantitatively presented as arbitrary units of fluorescence) from a given run were averaged separately, and then their ratio was used to describe the $\Delta\Psi_M$ properties of that sample.

Randy Tsen did all the modifications of LabView and Origin 7.0 programs.

2.5 Conclusion

The results presented in this chapter explain the preliminary experimental steps that we needed to develop in order to fulfill the requirements for monitoring subcellular properties on chip. We have also given the details of the mitochondria isolation procedure, which enabled us to compare the organelle properties in an isolated condition with the properties of mitochondria within cells.

Experiments in which we tested our initial experimental set-up clarified the necessary improvements of the equipment in order to monitor $\Delta\Psi_M$ on chip. The multi-wavelength detection system with appropriate sampling frequency, electronic filter and amplifier satisfied the requirements for obtaining good quality data.

The procedure we have used for mitochondria isolation was similar to the procedure from the Rabinowich lab [10], but was modified in many steps in order to make it work in our lab. One of the reasons for this was that the equipment from their lab (e.g. type of the centrifuges, rotors, homogenizers and tubes) differed from ours, so we had to adjust centrifuge-spinning parameters such as rpm and time of centrifugation. In order to adjust the isolation procedure correctly, we used information from general standard protocols [1-3, 11] as well as the experience we gained through the experimental work in the development of our protocol. We also added some details we found very useful such as using triethanolamine-acetate as the buffering system in order to weaken the cell membrane, or using a tight-fitting Dounce homogenizer for breaking cells and a loose-fitting Dounce homogenizer for proper cell suspension in the buffer.

2.6 Bibliography

1. Current Protocols in Cell Biology. Editors: JS Bonifacino, M Dasso, J Lippincott-Schwartz, JB Hardford and KM Yamada; **1999**: John Wiley &Sons, Inc.
2. Isolation of Cell Organelles, Cell Biology. Second adition ed. february **1992**.
3. Rickwood, D., M.T. Wilson, and V.M.D. Usmar, Mitochondria, a practical approach, ed. D.R.a.M.T.W. V.M. Darley Usmar. **1987**: IRL Press Limited, Oxford, England.
4. Bradford, M., A Rapid and Sensitive Method for the Quantification of Microgram Quantities of Protein Utilizing the Principle of Protein-Dye Binding. *Analytical Biochemistry*, **1976**. 72(May 7): p. 248-254.
5. Munujos, P., et al., Assay of Succinate Dehydrogenase Activity by a Colorimetric-Continuous Method Using Iodonitrotetrazolium Chloride as Electron Acceptor. *Analytical Biochemistry*, **1993**. 212: p. 506-509.
6. Salomon, A., et al., Structure-Acitvity Relationships within a Family of Selectively Cytotoxic Macrolide Natural Products. *Organic Letters*, **2000**. **0**(0): p. a-c.
7. Wang, C., et al., Integration of Immobilized Trypsin Bead Beds for Protein Digestion Within a Microfluidic Chip Incorporationg Capillary Electrophoresis Separations and an Electrospray Mass Spectrometry Interface. *Rapid Communications in Mass Spectrometry*, **2000**. 14: 1377-1383
8. Ocvirk, G., T. Tang, and D. Harrison, Optimization of Confocal Epifluorescence Microscopy for Microchip-Based Miniaturized Total Analysis Systems. *Analyst*, **1998**. 123: p. 1429-1434.
9. Zhonghui, H. and D. Harrison, Micromachining of Capillary Electrophoresis Injectors and Separators on Glass Chips and Evaluation of Flow at Capillary Intersections. *Analytical Chemistry*, **1994**. 66: p. 177-184.

10. Rabinovich, H., et al., A Role for Mitochondrial Bak in Apoptotic Response to Anticancer Drugs. *The Journal of Biological Chemistry*, **2001**. 276 (36): p. 34307-34317.

11. Fernandez-Vizzara, E., M. Lopez Perez, and E. JA, Isolation of Biogenetically Competent Mitochondria from Mammalian Tissues and Cultured Cells. *Methods*, **2002**. 26: p. 292-297.

12. Ramsey, J., et al., Flow Cytometry of Escherichia Coli on Microfluidic Devices. *Analytical Chemistry*, **2001**. 73: p. 5334-5338.

Chapter 3: Monitoring of Mitochondria Membrane Potential

3.1 Introduction

3.1.1 The Goal of Our Experiments

Our goal was to design and test a chip for flow cytometry. In order to test the quality of the new system, we chose to monitor the membrane potential of mitochondria ($\Delta\psi_M$), which is known to be the key element in apoptosis. The evaluation and regulation of this parameter is frequently used in current drug trials, and it has the potential to become even more important in the future. Our experiments focused on monitoring $\Delta\psi_M$ when treating intact Jurkat cells, or isolated mitochondria with a drug. The drugs chosen to induce apoptosis were valinomycin and oligomycin. The mechanism of their activity is different, so it is interesting to observe how they affect $\Delta\psi_M$ as a function of time and current reaction. We performed time response and dose response studies on chip and compared the results to those obtained using a flow cytometer. Establishing the detection technique on a microchip was the first step towards a better and more effective tool for future drug trials. In order to complete this task, it will still be necessary to integrate other analysis steps on a chip, so that mixing sample with the drugs, incubation, varying dose and staining can all be done automatically.

3.2 Experimental

3.2.1 Sample Preparation

Samples used in the experiments were either Jurkat cells or mitochondria isolated from the same cell line. Both cells and mitochondria were incubated with 10 μM valinomycin or 10 μM oligomycin and then stained with JC-1. Control groups of both cells and mitochondria were stained with JC-1, but did not receive the drug treatment.

After incubation with 10 μM valinomycin, Jurkat cells (1x 10^6 cells/mL) were centrifuged for 10 min. at 2000 rpm and resuspended in RPMI 1640 media. They were then stained with 10 μg/mL JC-1 for 10 min., washed twice and resuspended in phosphate buffered saline (PBS). Cells were then introduced into a microchip (channels 30 μm deep) or flow cytometer (Becton Dickinson, San Jose, CA, USA) for fluorescence detection. Mitochondria were isolated from Jurkat cells according to the protocol described in Chapter 2. Samples of 100 μl (protein concentration indicated in each experiment) stored at –70 °C were first thawed and then diluted to 1 ml by adding mitochondria buffer, MIB (10 mM MOPS adjusted with HCl to pH 7.4), 0.25 M sucrose (isotonic), 1 mM EDTA, 4 mM KH_2PO_4. Isolated mitochondria were incubated with 10 μM valinomycin or oligomycin for different periods of time, centrifuged 1 min at 13,000 rpm and resuspended in MIB. Then mitochondria were incubated with 10 μg/mL JC-1 stain for 1 min., washed twice, resuspended in PBS and then introduced into a microchip or flow cytometer for fluorescence detection. It is important to mention that isolated mitochondria were incubated with JC-1 stain for 2 min. in the earliest studies, which resulted in overloading the organelle with molecule of stain giving difficulties in setting the detector parameters. This was more noticeable in flow cytometry than in the chip experiments.

3.2.2 Experimental Procedure

3.2.2.1 Chip Experiments

We used the POCRE-chip design [1] with 30 μm deep channels for the experiments with cells, and 70 μm deep channels for experiments with mitochondria. The bigger channels were used with mitochondria due to their sticky nature, which caused clogging of smaller channels. Cells or mitochondria previously prepared for fluorescence detection were always introduced at a flow rate of 5 μL/min using negative pressure provided by a syringe pump (Harvard Apparatus, PHD 2000, Holliston, MA, USA) with a 100 μL SGE gas-tight syringe (Supelco, Bellefonte, PA, USA). All experiments in this section were performed with the multi-wavelength detection system described in Chapter 2. Photomultiplier (PMT) voltages for both red and green channels were set at 750 V for cells and 550 V for mitochondria experiment. Amplifier gains were 20x for red and 200x for green for mitochondria experiments, while cell experiments used 20x gain for both red and green fluorescence. Fluorescence signal was recorded for 10 seconds per run using a 5^{th} pole low pass filter of 100 Hz, a sampling frequency of 10,000 Hz and averaging of 4 data points, which gave a writing frequency of 2,500 Hz. Recorded data were analyzed in Origin 7.0 in the following way. The intensity of the red peak maximum in a 10 s run was averaged, as was the intensity of the green peaks coincident with the red peaks. The fluorescence signal was baseline corrected. The ratio of these values was used to obtain the red/green intensity ratio. The data presented are the average of 3-5 runs of 10 s. After each sample measurement and at the end of the experiment, microchip channels were thoroughly flushed with 70 % ethanol and then with mQ H_2O using house vacuum at the waste outlet.

3.2.2.2 Flow cytometry experiments

Samples were prepared for flow cytometry experiments in the same way as for chip experiments. Measurements were performed using a FACSort flow cytometer (Becton Dickinson, San Jose, CA, USA) equipped with an argon laser (488 nm). The instrument was calibrated before sample measurements. In order to analyze cells and isolated mitochondria stained with JC-1, compensation and PMT values for the detector in FL1 (green) and FL2 (red) were set as shown in the Table 3-1.

FACSort	cells	mitochondria
detector		
FL1(V)	280	360
FL2(V)	330	359
compensation		
FL1-%FL2	0.6	1.8
FL2-%FL1	34	9

Table 3-1. Flow cytometer parameters

Within only a few seconds, 50 000 events were acquired in each run. Means from the green and red peak fluorescence intensities were used to calculate the red/green fluorescence ratio. These values were used for comparison between different groups of samples and are plotted in the graphs.

3.3 Results and Discussion

3.3.1 Chip Studies

3.3.1.1 Pilot Experiments: Isolated Mitochondria Treated with Valinomycin

Both red and green fluorescence were recorded simultaneously using a multi-wavelength detection system. Data shown in Figure 3-1 present some of the first traces of red (a) and green (b) fluorescence obtained for mitochondria treated with valinomycin for 10 min. and stained with JC-1 for 2 min. Staining of mitochondria with a damaged membrane potential will show a drop in red fluorescence and either increased or unchanged green fluorescence, compared with healthy mitochondria [2]. Figures 3-1-c and -d show an expansion of a few peaks for red and green fluorescence. The figures clearly illustrate there are fewer high intensity green peaks than red peaks. It can also be seen that the green peaks are coincident with the red peaks. Estimated peak width for this experiment was 1 ms, which was much narrower compared to the obtained peak base width of about 10-15 ms and FWHP of about 5 ms. This peak broadening was caused by the 100 Hz low pass filter but the peaks were not overlapped, which gave acceptable quality data.

In conclusion, the results from this section show that the microchip with a multi-wavelength detection system worked well, so we could proceed with time response and dose response experiments.

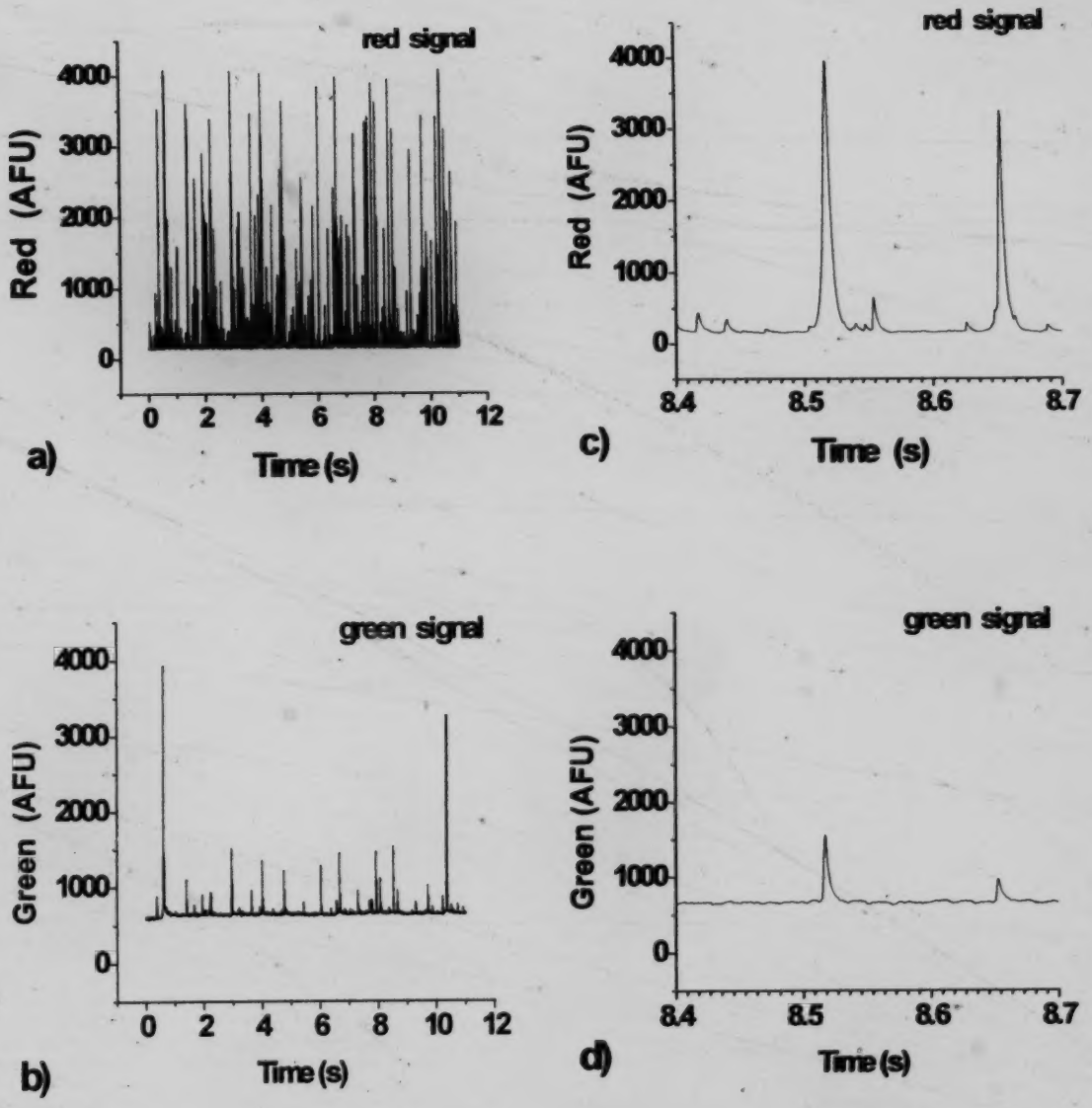

Figure 3-1. Red and green fluorescence vs. time. One of the first results showing simultaneously red (**a**) and green trace (**b**) of isolated mitochondria, crude preparation (protein concentration 2 mg/mL; final protein concentration in the sample 0.2 mg/mL) treated with 10 μM valinomycin for 10 min; Figures (**c**) and (**d**) show expansions of 0.3 s from Figures (**a**) and (**b**) respectively.

3.3.1.2 Mitochondria/Cells Comparison

In this section, we have compared the effect of 10 μM valinomycin on isolated mitohochondria and mitochondria in Jurkat cells (1 x 10^6 cells/mL). A 100 μL aliquot of mitochondria isolated on a Percoll gradient (fraction B, protein concentration of 0.49 mg/mL, see Chapter 2 Section 2.4.1) was diluted to 1 mL by adding MIB, resulting in a final protein concentration of 0.049 mg/mL. Both cells and isolated mitochondria were exposed to 10 μM valinomycin for 10 min. The incubation time with JC-1 stain was 10 min. for cells and 2 min. for mitochondria. Figure 3-2 shows individual traces of red and coincident green fluorescence from both healthy and drug-treated isolated mitochondria. The drop in the red/green fluorescence ratio is proportional to the damage to the mitochondrial membrane potential.

The results in Figure 3-3 represent average values of red/green fluorescence intensity for 5 runs. Results for both cells and isolated mitochondria are shown, error bars are standard deviations. The data illustrate that isolated mitochondria are more susceptible to valinomycin than mitochondria within a whole cell. The red/green fluorescence ratio droped 60 % for mitochondria within a whole cell and 75 % for isolated mitochondria. Mitochondria within an intact cell may be healthier, because they did not undergo the isolation procedure. However, the most likely reason for the greater susceptibility of isolated mitochondria to valinomycin is that in intact cells, the drug must first penetrate the outer cell membrane.

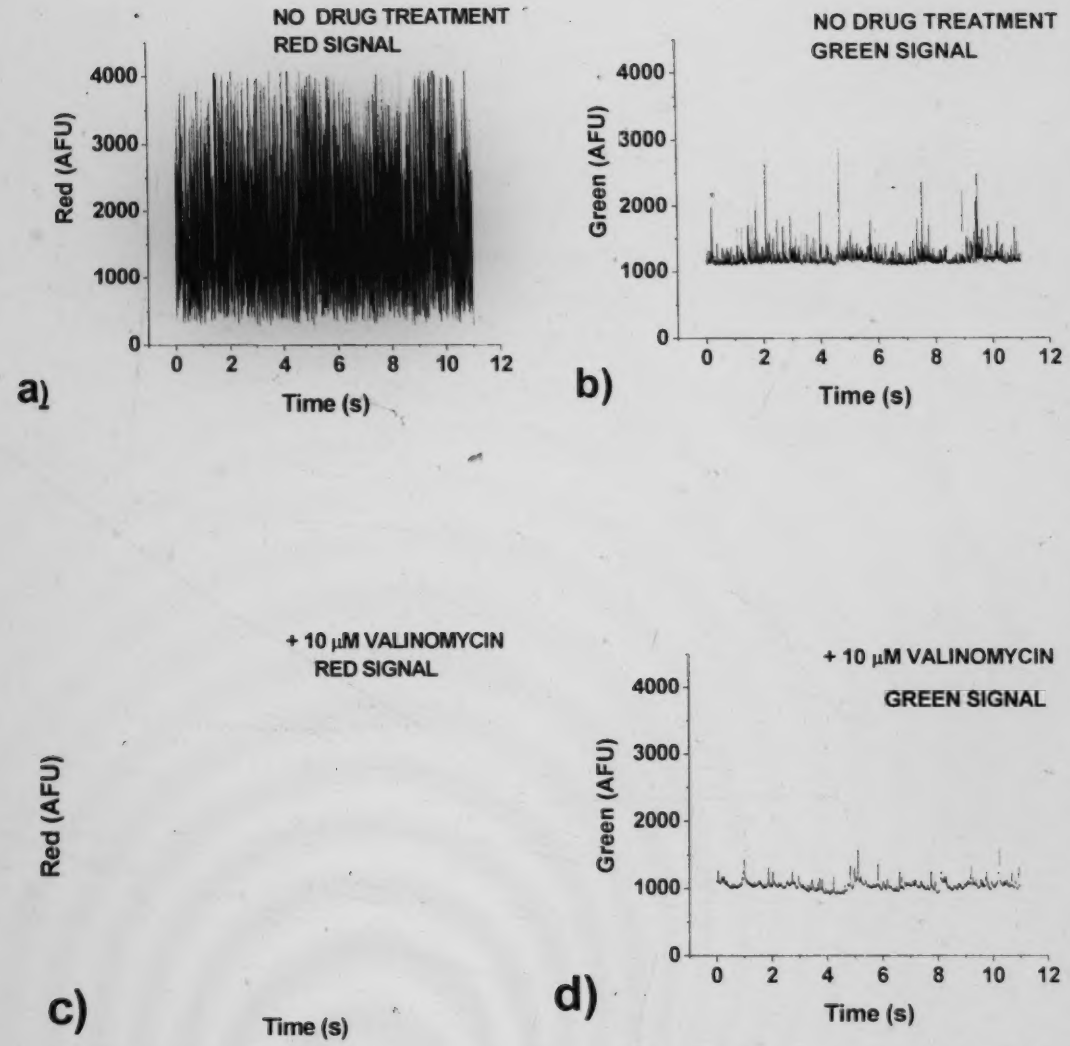

Figure 3-2. Traces of red and green fluorescence where a) and b) represent signal for the control group (mitochondria not treated with the drug), while c) and d) show recorded signals for treated mitochondria. Final protein concentration of mitochondria samples was 0.05 mg/mL. Mitochondria were treated with 10 μM valinomycin for 10 min. and then stained with J,4033,1415,4031,1415,4029,1415,4027,1415,4025,1415,4021,1415,401

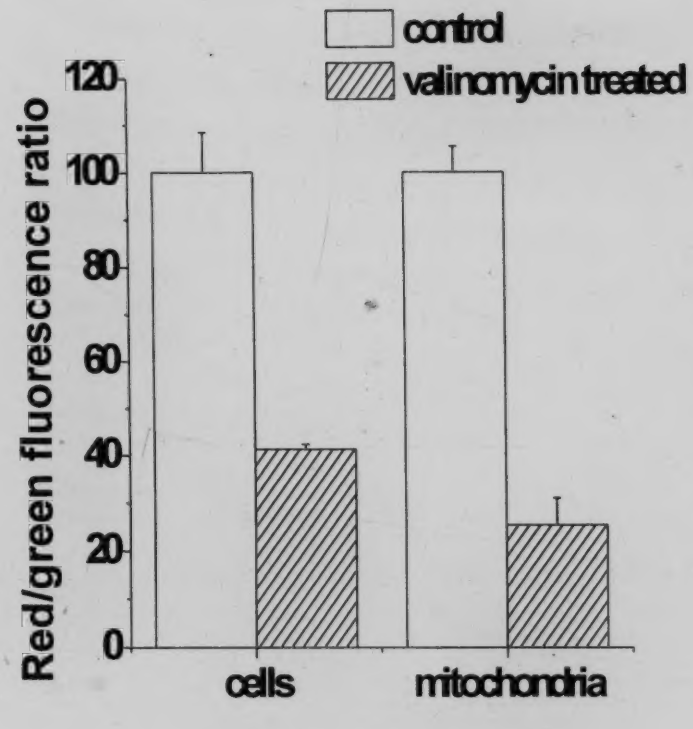

Figure 3-3. Comparison of data between intact cells and isolated mitochondria. Figure shows a 75 % decrease in red/green fluorescence ratio for Percoll isolated mitochondria (protein concentration 0.05 mg/mL) and 60 % decrease for Jurkat cells (1 x 10^6 cell/mL) after they were treated with 10 μM valinomycin for 10 min.

3.3.1.3 Comparative Dose Response Study for Two Drugs

We compared the dose response of the mitochondria membrane potential to two drugs: valinomycin and oligomycin. Mitochondria sample (crude preparation, final protein concentration of 0.2 mg/mL) was incubated with 0 μM, 10 μM, 50 μM and 100 μM drug. Then it was stained with 10 μg/mL JC-1 for 1 min. and introduced into a chip at a flow rate of 5 μL/min. The results in Figure 3-4 show the red/green fluorecence ratio plotted against the correspondent drug concentration in four individual experiments.

The values are normalized to set the healthy cell, red/green ratio equal to 100. We have shown individual experiments instead of the mean values of several trials. The standard deviation bars shown in the Figure 3-4 represent the instrumental error, which is much smaller than the variation arising from the biological sample preparation. Handling a biological sample involves a series of steps, such as cell preparation, pipetting, staining and centrifugation, which all introduce variations. Small differences in the timing of these steps, or in the age and state of the biological components, may explain the differences in the red/green fluorescence ratio between different trials done with the same dose of drug.

In Figure 3-4, a pair of trials (exp.1) obtained on the same day for both oligomycin and valinomycin is shown. By using mitochondria of approximately the same age and history we hoped to obtain the most representative data. Comparisons within each trial show a difference between the effect of the valinomycin and oligomycin. However, the large variations from trial to trial create large deviations. This problem was seen throughout all of our experiments on both chip and FACSort systems. Unfortunately, those comparison runs could not be done with the same sample on the same day.

The results in Figure 3-4 show that there is a depolarization of mitochondria membrane after treatment with both valinomycin and oligomycin. Valinomycin shuttles K^+ through the mitochondria membrane to the mitochondrial matrix and directly affects $\Delta\psi_M$ in that way. In the literature, it is confirmed that this ionophore always causes $\Delta\psi_M$ to drop, disregarding the cell type [3-7]. In addition, $\Delta\psi_M$ drop is more evident with the addition of K^+ ions. Oligomycin inhibits the oxidative phosphorylation by blocking

F_oF_1ATP-ase, which is involved in ATP synthesis [8]. Oligomycin binds to the F_o unit of F_oF_1ATP-ase, preventing H^+ transfer to the mitochondrial matrix, causing hyperpolarization of the mitochondria membrane (increase in $\Delta\psi_M$) [2]. Unlike valinomycin, oligomycin will affect $\Delta\psi_M$ differently for different cell types, suggesting different mechanisms in generating $\Delta\psi_M$ [9]. For example, Kalbacova and coworkers monitored $\Delta\psi_M$ of BSC-40 cells and Hela cells treated with the same concentration of oligomycin. They observed a moderate decrease of $\Delta\psi_M$ in HeLa cells and an increase in BSC-40 cells, which led to the conclusion that BSC-40 cells are more sensitive than Hela to inhibitors of oxidative phosphorylation. There are no reports about the affect of oligomycin on Jurkat cells, except in combination with Fas-activating antibody, when it fascilitates cell death and causes $\Delta\psi_M$ to drop [10, 11]. As our data show a moderate drop of $\Delta\psi_M$ in Jurkat cells, we can conclude that Jurkat cells are not directly affected by oligomycin, and $\Delta\psi_M$ drop can be explained as a consequence of general changes in mitochondria functions triggered by inhibition of oxidative phosphorylation.

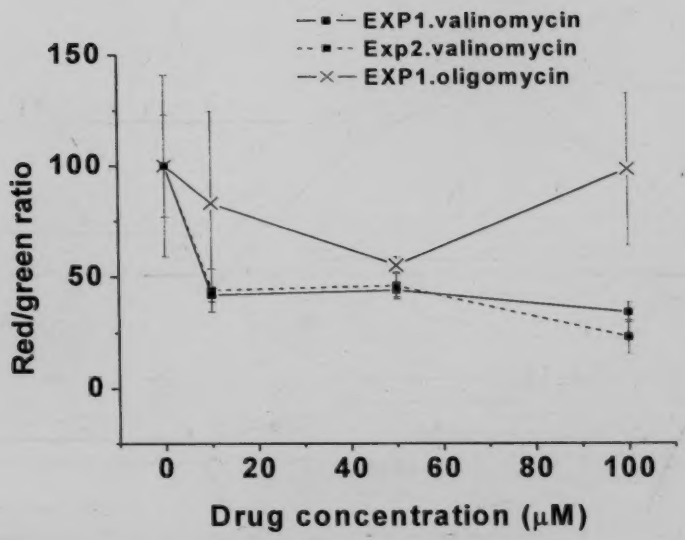

Figure 3-4. Dose response studies; three experiments shown. Crude isolated mitochondria (protein concentration 0.2 mg/mL) were incubated with valinomycin or oligomycin for 10 min and then stained with JC-1 (incubation time 1 min.). The ratio of red/green fluorescence intensity is plotted in the graph against drug concentration. The sample was introduced into a microchip of 70 μm deep channels at a flow rate of 5 μL/min.

Chip experiments	Red/green fluorescence ratio				
Drug conc. (μM)		0	10	50	100
Valinomycin	exp.1	100	44	46	23
	exp.2	100	42	44	34
Oligomycin	exp.1	100	83	55	98

Table 3-2. Dose response studies; values shown in Figure3-4

A scatter plot of the individual peaks for red vs. green fluorescence values provides another way to evaluate the change in fluorescent intensities. Figure 3-5 shows approximately 1000 events occurring during a 10 s run, demonstrating a shift in green fluorescence toward higher values and a decrease in red fluorescence, which indicates depolarization of mitochondria membrane. The same comments apply as in section 3.3.1.3.

These data demonstrate the ability of our system and software to graphically represent and analyze the data in the same fashion as a flow cytometer, although there is a smaller number of events (1,000- chip vs. 50,000- flow cytometer).

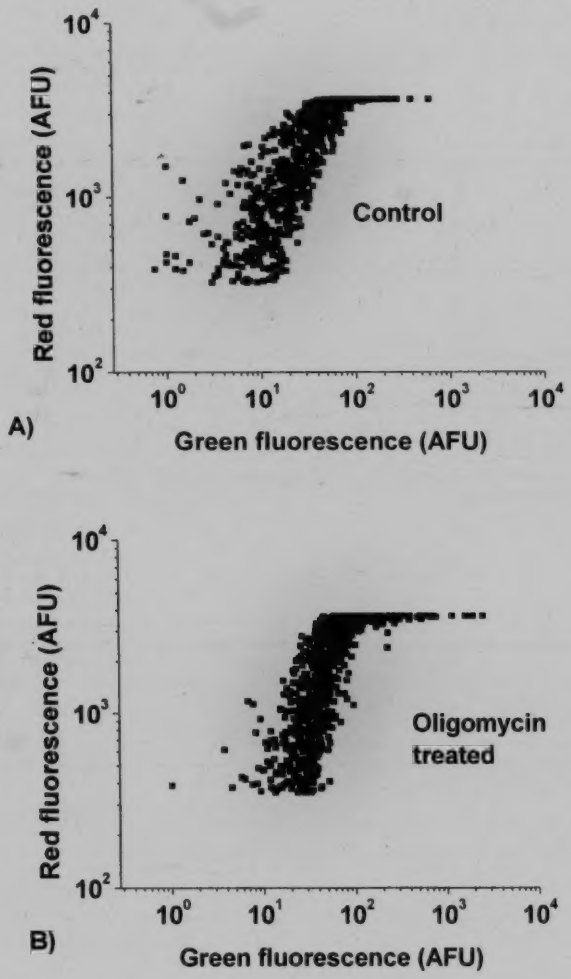

Figure 3-5. Scattering plots of red vs. green fluorescence for isolated mitochondria (crude preparation with final protein concentration of 0.2 mg/mL) treated with 100 μM oligomycin for 10 min (a) and not treated with oligomycin (b). Sample was then stained with JC-1 stain (incubation time 1 min.). The graphical analysis and representation of the data was done in Origin 7.0.

3.3.2 Flow Cytometry Studies

3.3.2.1 Comparative Dose Response Study for Two Drugs

Several studies were undertaken to compare the microchip system with a flow cytometer. Dose response studies with two drugs performed with the microchip were compared to the results obtained by flow cytometry. In these experiments, we treated a crude preparation of mitochondria sample (final protein concentration of 0.2 mg/mL) with 0, 50, or 100 μM drug for 10 min. Fully damaged or dead mitochondria were obtained by exposure to 95 ± 5 °C for 10 min. Mitochondria were then stained with JC-1 for 1 min. Each symbol in Figure 3-6 represents the average value from the two experiments. Ratios are normalized to set the value for healthy cells to 100. Large standard deviations are attributed to variations in the biological sample preparation, as discussed earlier. The results of this comparative dose response study for valinomycin and oligomycin show that valinomycin damages $\Delta\psi_M$ to a greater extent at a given dose than does oligomycin.

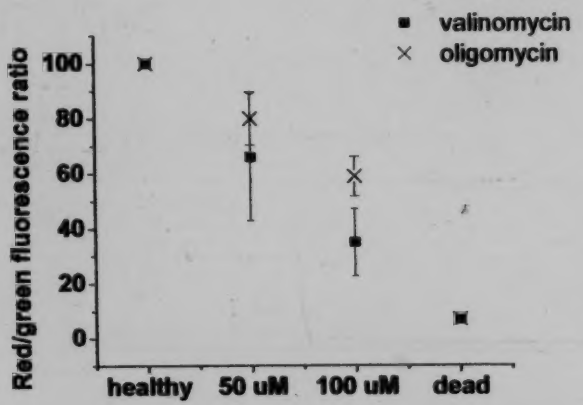

Figure 3-6. Comparative dose response for valinomycin and oligomycin; standard deviation for healthy mitochondria is represented by the size of the symbol; the size of the symbol for dead mitochondria represents the range, not the standard deviation. Dead mitochondria are killed by heat (10 min. in water bath at 95 ± 5 °C) and then stained with JC-1.

Flow cytometry data in Figure 3-7 show individual scatter plots of red vs. green fluorescence for mitochondria treated with either valinomycin, oligomycin or heat (95 ± 5 °C) for 10 min. All the experimental conditions are the same as in Figure 3-6. Plots represent experiments with 50,000 events. Similar to the chip scatter plots, there is a shift of red fluorescence toward lower intensity, while green fluorescence is increased. The results, showing a drop in red fluorescence for valinomycin are in agreement with data published by Cossariza et al. [3-5]

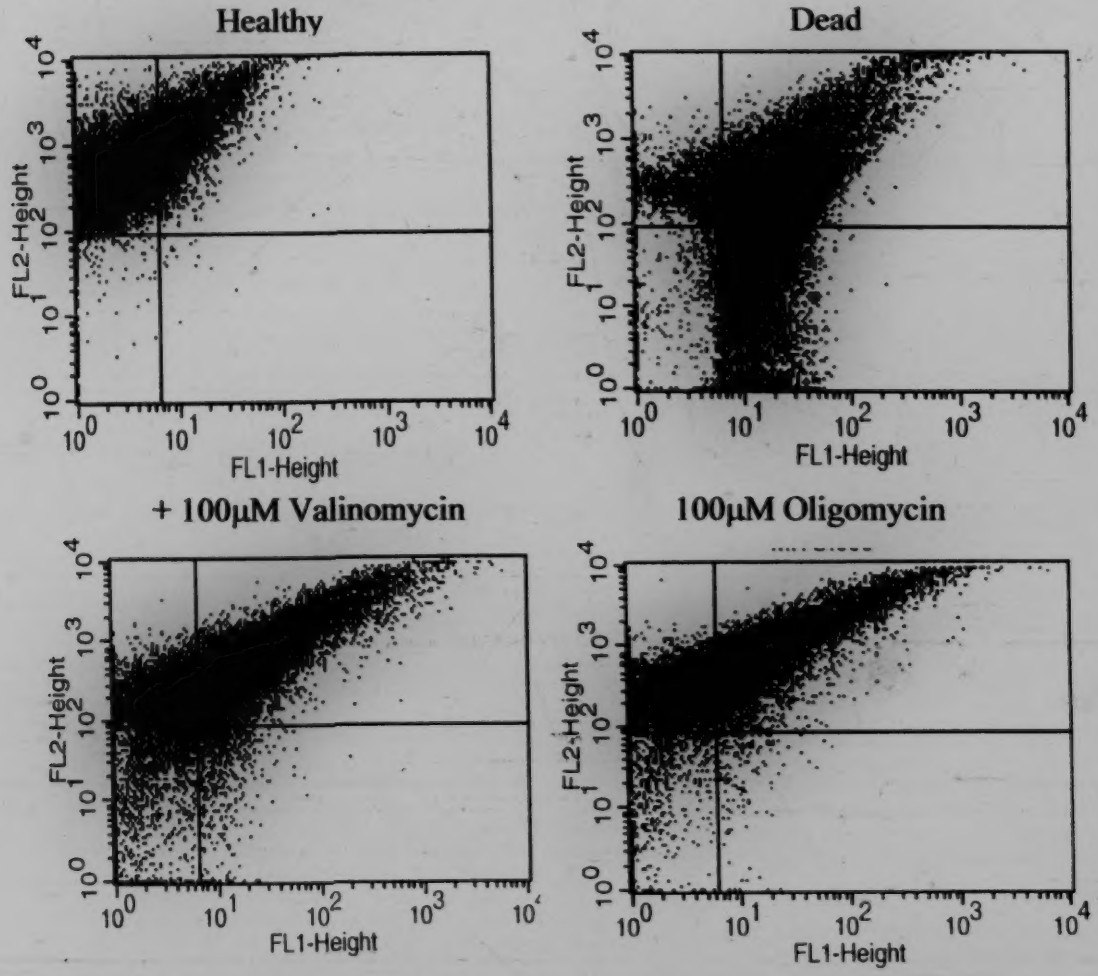

Figure 3-7. Scatter plots of red vs. green fluorescence from comparative dose response study. Mitochondria samples are incubated with 100 μM drug or exposed to heat (95 ± 5 °C) for 10 min and compared with non-treated mitochondria after staining with JC-1 stain. FL-1 and FL-2 are green and red fluorescence, respectively.

3.3.3 Microchip/ Flow Cytometry Comparison

3.3.3.1 Time Response Study with Cells and Valinomycin

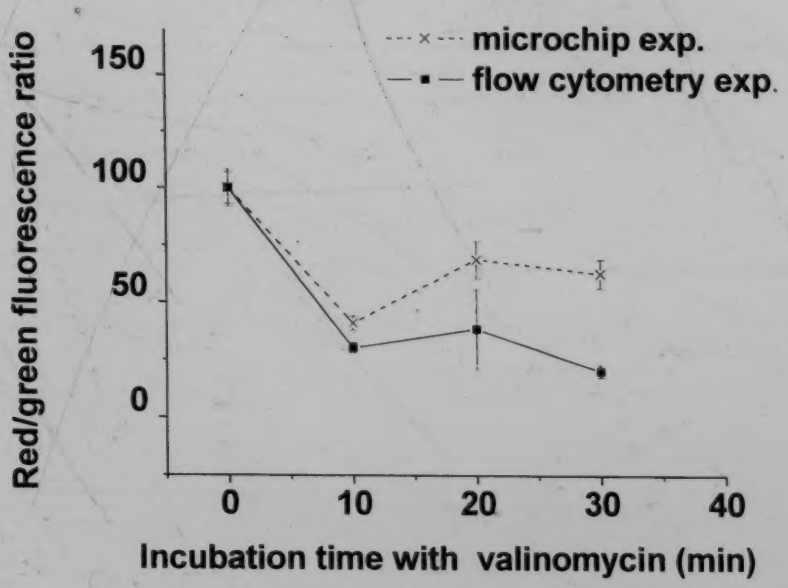

Figure 3-8. Comparative time response study done with microchip and flow cytometer. Cells were treated with valinomycin for different periods of time and stained with JC-1 stain

An incubation time response study was performed with intact Jurkat cells (1 x 10^6 cells/mL) that were incubated with 10 μM valinomycin for 10, 20 and 30 min., stained with 10 μg/ mL JC-1 for 2 min. and then compared with non-treated cells. The red/green fluorescence ratio was measured by a flow cytometer and a microchip. The data in Figure 3-8 demonstrate that these two detection methods give similar results. Numerical values for the red/green fluorescence ratio are shown in Tables 3-3 and 3-4.

Tables 3-3 and 3-4 show numerical values for red/green fluorescence ratios from Figure 3-8. To facilitate comparison, data were normalized to 100 for the control sample, which was not treated with the drug.

Flow cytometer	Red/green	ratio	shown in	Figure 3-8
Incub. time	0min	10min	20min	30min
Exp.1	5.59	1.52	2.7	1
Exp.2	5.07	1.68	1.38	1.2
Average	5.33	1.6	2.04	1.1
Stdev	0.37	0.11	0.93	0.14
Figure values	**100**	**30**	**38.3**	**20**
	6.9	**2.1**	**17.4**	**2.62**

Table 3-3. Time response study; flow cytometry experiment

Microchip	Red/green	ratio	shown in	Figure 3-8
Incub. time	0min	10min	20min	30min
Exp. 1	5.59	1.52	2.7	1
Average	5.59	1.52	2.7	1
Stdev (instr. error)	0.37	0.11	0.93	0.14
Figure values	**100**	**30**	**38.3**	**20**
	6.9	**2.1**	**17.4**	**2.62**

Table 3-4. Time response study; microchip experiment

3.3.3.2 Dose Response Study with Isolated Mitochondria and Two Drugs

3.3.3.2.1 Mitochondria Treated with Valinomycin

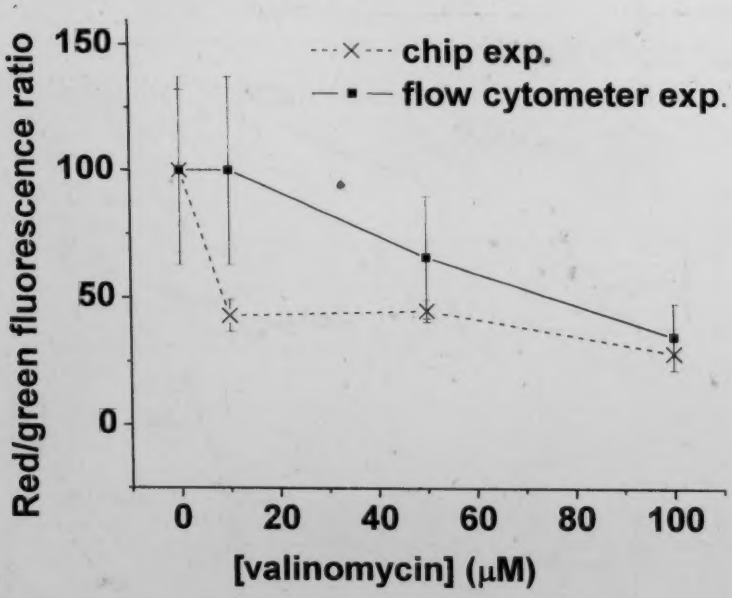

Figure 3-9. Comparative dose response study for microchip and flow cytometry experiments performed with isolated mitochondria treated with valinomycin for different periods of time.

Figure 3-9 shows a comparative dose response study for isolated mitochondria (crude preparation; final protein concentration in the sample was 0.2 mg/mL) treated with 10, 50 and 100 μM valinomycin for 10 min. and stained with JC-1 for 1 min. Sample was then introduced into a microchip or flow cytometer for fluorescence detection. Values shown in the figure represent average values for three flow cytometry and two chip experiments. Each study was performed on a different day. Large standard deviations are due to the variation in the biological samples, as discussed above. Results are normalized to 100 for healthy mitochondria.

3.3.3.2.2 Mitochondria Treated with Oligomycin

A comparison of the chip and flow cytometer was also made for a dose response study of oligomycin, using a crude preparation of mitochondria (final protein concentration of 0.2 mg/mL). The sample is treated with 10, 50 and 100 μM oligomycin for 10 min., stained with JC-1 then introduced into the microchip or flow cytometer. The data shown in Figure 3-10 represent average values for three flow cytometry and two microchip experiments, each performed on a different day. Results are normalized to 100 for healthy mitochondria.

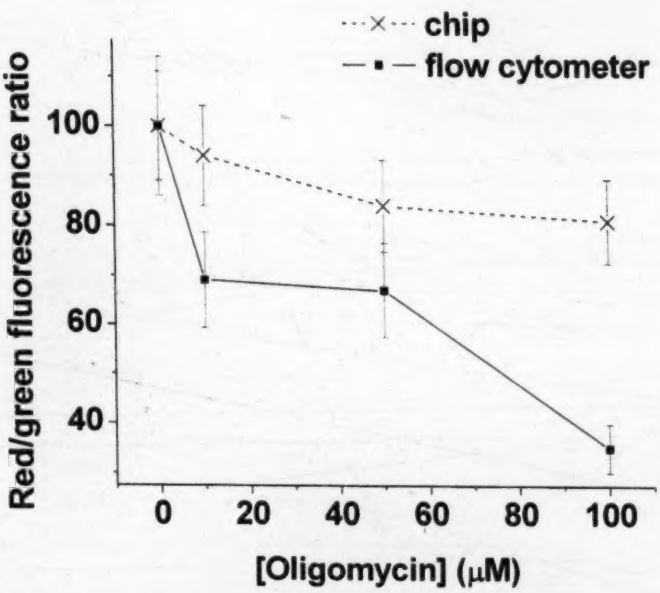

Figure 3-10. Dose response study performed with isolated mitochondria (protein concentration of 0.2 mg/mL) and oligomycin. Data shown represent the average values for 3 flow cytometry and 2 chip experiments.

The data shown in Figure 3-11 show a comparison between values of the red/green fluorescence ratio for only one flow cytometry and one chip experiment. This comparison shows it is possible to obtain essentially identical results with the two methods. However, as Figure 3-10 illustrates, the variability in sample is quite large, making quantitative comparison of the two methods somewhat difficult. Nevertheless, comparison of the red/green ratio drop for mitochondria treated with oligomycin appears to give comparable values for both chip and flow cytometry techniques.

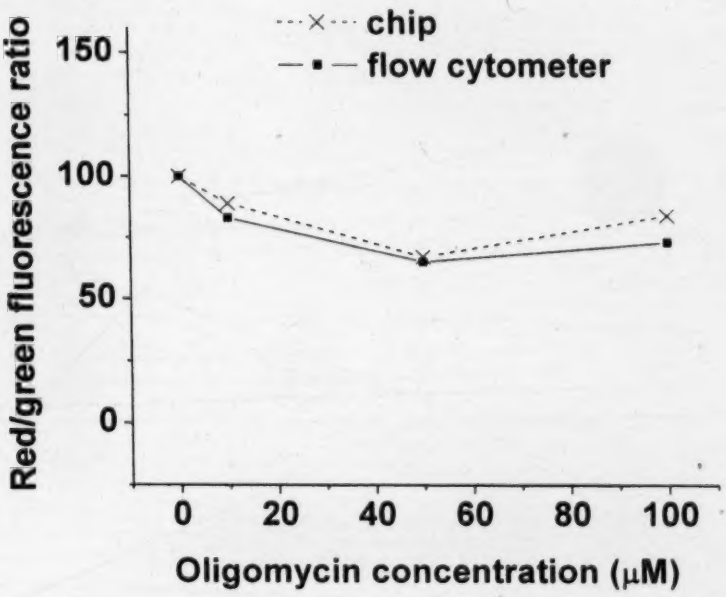

Figure 3-11. Dose response study with oligomycin; one flow cytometry and one chip experiment

3.4 Conclusion

This study has used the comparison of the effect of two drugs as a vehicle to compare two instrumentation techniques: microchip system and conventional flow cytometry. We have succesfully performed time response and dose response studies using valinomycin and oligomycin both on a microchip and on flow cytometer. Our experiments illustrate that both valinomycin and oligomycin induce a drop in $\Delta\psi_M$ in Jurkat cells and valinomycin does so in lower doses. The expected hyperpolarization of mitochondria membrane was not observed, which suggests that the mechanism of $\Delta\psi_M$ generation in Jurkat cells most likely does not depend much on the activity of F_oF_1ATPase.

In all the cases where data represented average values from two or more experiments, there were large standard deviations. Some variation in the preparation of the biological samples was the source of this large experimental error. The deviations could have been reduced and the comparison would have been more accurate if we had had the opportunity to measure the same sample by two techniques at the same time. Supporting this perspective, examination of individual experiments, such as Figure 3-4 and Figure 3-11, shows much smaller standard deviations caused by instrumental error alone. We conclude that the red/green ratio drop for mitochondria treated with drug gave comparable values for both chip and flow cytometry experiments. Our results also demonstrate that it is possible to obtain the same data using either the microchip equipped with a multi-wavelength detection system or a flow cytometer.

In order to improve the microfluidic system further, there are several changes that could be made. The chip design could be adjusted to be more similar to the design of the flow cytometer through the use of sheath flow on chip. We should also address channel size and the adherence of biological sample on the microchannel walls. For cells, a microchip with 30 μm channel depth was used, yet the smaller particles (isolated mitochondria) required 70 μm deep channels. This was because the mitochondria and cell debris are extremely sticky, causing clogging of smaller channels. However, these bigger

channels caused a higher probability of detecting multiple particles simultaneously. In order to overcome this problem in the future, channels might be coated to prevent sticking of the debris to channel walls. One of the suggested solutions might be coating with fetal calf serum, which has been shown to prevent cells from sticking to the channel walls [12].

Monitoring $\Delta\psi_M$ using flow cytometer has been a conventional technique for some time. The flow cytometer is a stable system with high sensitivity, and it collects about ten times more data than a microchip system. But there might be an advantage in using microchips over a flow cytometer in the future. This advantage lies in the integration of preparative steps for the biological samples within the detection system. This whole complex process may be performed on chip, integrating drug treatment, staining, washing and finally detection of the fluorescence signal. The integration would reduce the total analysis time and it would also exclude human errors, which may contribute to the large deviation in day-to-day analysis.

3.5 Bibliography

1. Fluri, K., et al., Integrated Capillary Electrophoresis Devices with an Efficient Postcolumn Reactor in Planar Quartz and Glass Chips. *Analytical Chemistry*, **1996**. 68: p. 4285-4290.
2. Pon, L. and E. Schon, Mitochondria. *Methods in Cell Biology*, **2001**. 65.
3. Cossariza, A., et al., A New Method for the Cytofluorimetric Analysis of Mitochondrial Membrane Potential Using J-Agregate Forming lipophilic Cation 5, 5',6,6'-tetrachloro-1,1'3,3'-tetraethylbenzimidazolcarbocynanine Iodide (JC-1). *Biochemical and Biophysical Research Communications*, **1993**. 197(1): p. 40-45.
4. Cossariza, A., et al., Mitochondrial Modifications during Rat Thymocyte Apoptosis: A Study at the Single Cell Level. *Experimental Cell Research*, **1994**. 214: p. 323-330.
5. Cossariza, A., D. Ceccarelli, and A. Masini, Functional Heterogeneity of an Isolated Mitochondria Population Revealed by Cytofluorimetric Analysis at the Single Organelle Level. *Experimental Cell Research*, **1996**. 222: p. 84-94.
6. Ludovico, P., F. Sansonetty, and M. Corte-Real, Assesment of Mitochondrial Membrane Potential in Yeast Cell Populations by Flow Cytometry. *Microbiology*, **2001**. 147: p. 3335-3343.
7. Petit, P., et al., Analysis of the Membrane Potential of Rat and Mouse-Liver Mitochondria by Flow Cytometry and Possible Applications. *European Journal of Biochemistry*, **1990**. 194: p. 389-397
8. Voet, D. and J. Voet, *Biochemistry*. **1990**: John Wiley & Sons
9. Kalbacova, M., et al., Comparison of the effect of Mitochondrial Inhibitors on Mitochondrial Membrane Potential in Two Different Cell Lines Using Flow Cytometry and Spectrofluorometry. *Cytometry Part A*, **2003**. 52A: p. 110-116.

10. Tirosh, O., A. Aronis, and A. Melendez, Mitochondrial state 3 to 4 respiration transition during Fas-mediated apoptosis controls cellular redox balance and rate of cell death. *Biochemical Pharmacology*, **2003**. 66: p. 1331-1334.

11. Aronis, A., et al., Potentiation of Fas mediated apoptosis by attenuated production of mitochondria-derived reactive oxygen species. *Cell Death and Differentiation*, **2003**. 10(3): p. 335-344

12. Salimi-Moosavi, H., et al., Biology Lab-on-a-Chip for Drug Screening. *Micro Total Analysis Systems*, **1998**: p. 69-72.

Chapter 4: Summary

4.1 Summary

This chapter summarizes the work presented in Chapter 2 and Chapter 3 and gives some thoughts on future directions for the continuation of research in the same area.

In Chapter 2, we have presented the preliminary experimental steps necessary for providing appropriate equipment for data acquisition in the experiments for monitoring $\Delta\psi_M$. Our efforts resulted in a multi-wavelength detection system with a sampling frequency, electronic filter and amplifier adequate for collecting data of good quality. A second major task was accomplished by developing the protocol for isolation of mitochondria from Jurkat cells. The protocol that worked well in our lab was a modification of a few others [1-5], from which we primarily used the procedures of reference [1].

In Chapter 3, the microchip system and a conventional flow cytometry technique were compared, performing time response and dose response studies with two drugs: valinomycin and oligomycin. The data obtained in the experiments show large variations, which we attribute to the preparation of the biological sample. Single experiment data support this argument, showing only instrumental error, which was fairly small. In spite of the fact that there was not an opportunity to measure the same sample simultaneously with both techniques, the results demonstrate that a chip with the multi-wavelength detection system gave values for red/green fluorescence ratios that were comparable to those obtained by flow cytometer.

Regarding future work, there are a few suggestions, which could lead toward the improvement of the system and easier handling of biological samples in a microfluidic device. It would be advisable to do some additional work on chip redesigning in order to enable sheath flow in microchannels, as was done in Ramsey's group [6]. This would better imitate flow cytometry and possibly offer better basic microfluidic devices, which could further be upgraded to integrate preparation steps for biological samples (staining, drug dilution with buffers, drug exposure etc.). One of the problems addressed in our

work was related to the adherence of isolated mitochondria to the walls of microchannels. Although, 30 μm deep channels seemed too large for mitochondria of a 1 μm size, we had to switch to 70 μm deep channels, because sticky cell debris from mitochondria preparation quickly clogged 30 μm deep channels. We have proposed channel coating with fetal calf serum, which worked well for preventing human neutrofils and lymhocytes adhesion on channel walls [7]. It further remaines to examine if this effect will be the same for isolated mitochondria. Following the assumption that this problem originates from the protein content that is present in the sample, it might be very useful to examine the adherence rate of the different mitochondria fractions isolated on Percoll gradient. These fractions have considerably lower protein content compared with crude mitochondria, which were more often used in our experiments.

4.2 Bibliography

1. Rabinovich, H., et al., A Role for Mitochondrial Bak in Apoptotic Response to Anticancer Drugs. The Journal of Biological Chemistry, 2001. 276 (36): p. 34307-34317.
2. Rickwood, D., M.T. Wilson, and V.M.D.-. Usmar, Mitochondria, a practical approach, ed. D.R.a.M.T.W. V.M. Darley Usmar. Vol. l. 1987: IRL Press Limited, Oxford, England.
3. Current Protocols in Cell Biology. 1999: John Wiley &Sons, Inc.
4. Isolation of Cell Organelles, Cell Biology. Second adition ed. february 1992.
5. Fernandez-Vizzara, E., M. Lopez Perez, and E. JA, Isolation of Biogenetically Competent Mitochondria from Mammalian Tissues and Cultured Cells. Methods, 2002. 26: p. 292-297.
6. Ramsey, J., et al., Flow Cytometry of Escherichia Coli on Microfluidic Devices. Analalytical Chemistry, 2001. 73: p. 5334-5338.
7. Salimi-Moosavi, H., et al., Biology Lab-on-a-Chip for Drug Screening. Micro Total Analysis Systems, 1998: p. 69-72.

Appendix

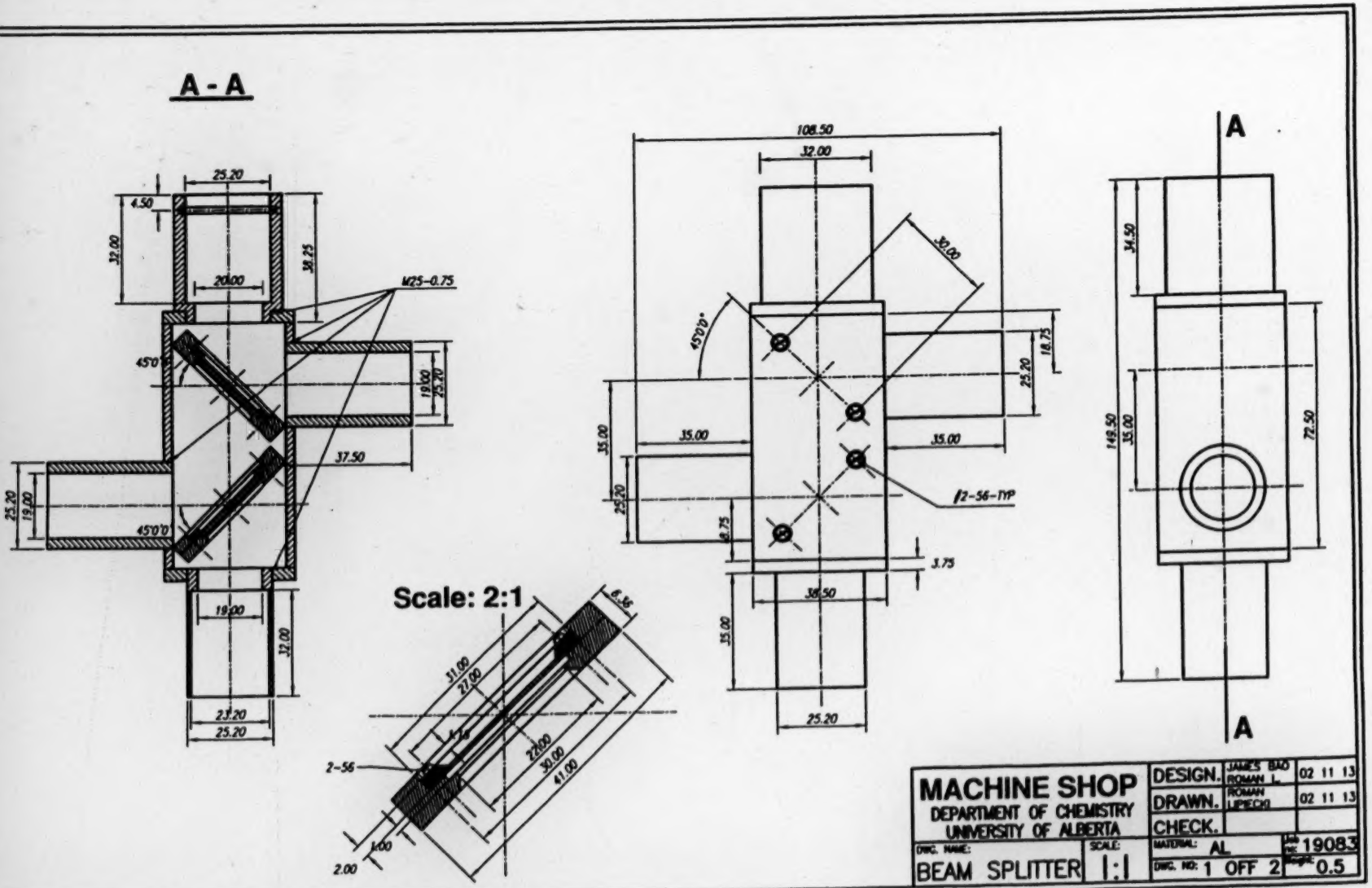
A - A
25.20
4.50
32.00
20.00
38.25
M25-0.75
45°D
19.00
25.20
37.50
23.20
19.00
45°D
19.00
32.00
23.20
25.20
Scale: 2:1
6.35
31.00
27.00
4.76
2-56
22.00
30.00
41.00
1.00
2.00
108.50
32.00
32.00
45°D
18.75
25.20
35.00
35.00
35.00
2-56-TYP
9.75
3.75
38.50
35.00
25.20
A
34.50
149.50
35.00
72.50
A
MACHINE SHOP
DEPARTMENT OF CHEMISTRY
UNIVERSITY OF ALBERTA
DESIGN.
JAMES BAO
ROMAN L.
02 11 13
DRAWN.
ROMAN LIPECKI
02 11 13
CHECK.
DWG. NAME:
BEAM SPLITTER
SCALE:
1:1
MATERIAL:
AL
DWG. NO: 1 OFF 2
Job No. 19083
Weight 0.5